© 2019. Published by The Company of Biologists Ltd | Development (2019) 146, dev174623. doi:10.1242/dev.174623

RESEARCH ARTICLE

A cadherin switch marks germ layer formation in the diploblastic sea anemone *Nematostella vectensis*

Ekaterina A. Pukhlyakova[1], Anastasia O. Kirillova[1,2,*], Yulia A. Kraus[2], Bob Zimmermann[1] and Ulrich Technau[1,‡]

ABSTRACT

Morphogenesis is a shape-building process during development of multicellular organisms. During this process, the establishment and modulation of cell-cell contacts play an important role. Cadherins, the major cell adhesion molecules, form adherens junctions connecting epithelial cells. Numerous studies of Bilateria have shown that cadherins are associated with the regulation of cell differentiation, cell shape changes, cell migration and tissue morphogenesis. To date, the role of cadherins in non-bilaterians is unknown. Here, we study the expression and function of two paralogous classical cadherins, Cadherin 1 and Cadherin 3, in a diploblastic animal, the sea anemone *Nematostella vectensis*. We show that a cadherin switch accompanies the formation of germ layers. Using specific antibodies, we show that both cadherins are localized to adherens junctions at apical and basal positions in ectoderm and endoderm. During gastrulation, partial epithelial-to-mesenchymal transition of endodermal cells is marked by stepwise downregulation of Cadherin 3 and upregulation of Cadherin 1. Knockdown experiments show that both cadherins are required for maintenance of tissue integrity and tissue morphogenesis. Thus, both sea anemones and bilaterians use independently duplicated cadherins combinatorially for tissue morphogenesis and germ layer differentiation.

KEY WORDS: Cadherin, Cell adhesion, Morphogenesis, Germ layers, *Nematostella*, Cnidaria

INTRODUCTION

Morphogenesis is a process of tissue and organ formation during organism development (Gilbert, 2013) that is driven by coordinated cell shape changes, cell migration, cell proliferation, cell death and cell adhesion. The key morphogenetic events during early development are gastrulation, germ layer formation, folding of the neural tube and body axis elongation. Cadherins are transmembrane cell adhesion molecules that play an important role in these processes. They not only provide the mechanical connection between cells, but also control cell-cell recognition, cell sorting, tissue boundary formation, signal transduction, formation of cell and tissue polarity, cell migration, cell proliferation and cell death (Gumbiner, 2005; Halbleib and Nelson, 2006). In adult tissues, cadherins preserve stable and ordered tissue integrity (Angst et al., 2001; Halbleib and Nelson, 2006).

Classical cadherins are conserved molecules present in all animals whose genomes have been analyzed (Alberts, 2007). They are major components of the adherens junctions between cells, which are conserved structures of epithelial cells in most animals (Meng and Takeichi, 2009). In adherens junctions, cadherins form homophilic (more rarely heterophilic) calcium-dependent interactions with other cadherin molecules from neighboring cells. The cytoplasmic domain of cadherins is highly conserved among metazoans, distinguishing classical cadherins from other cadherin subfamilies (Hulpiau and van Roy, 2011; Oda and Takeichi, 2011). The cytoplasmic domain contains β-catenin and p120 binding sites. Catenins connect cadherins with the actin cytoskeleton in a dynamic manner (Meng and Takeichi, 2009). In comparison with other cadherin subfamilies, classical cadherins are unique in that they show the most noticeable variation in their extracellular region among different species (Hulpiau and van Roy, 2011). Indeed, the extracellular domain consists of a variable number of cadherin repeats of about 110 amino acids each and, depending on the species, laminin G and epidermal growth factor (EGF)-like domains.

During development, the regulation of specific cadherin expression correlates with the formation of new tissues. For instance, folding of the neural tube in vertebrates occurs in parallel with downregulation of epithelial cadherin (E-cadherin) and upregulation of neuronal cadherin (N-cadherin) (Nandadasa et al., 2009). Such cadherin switches are characteristic of several different morphogenetic processes, such as gastrulation and neural crest development (Basilicata et al., 2016; Dady et al., 2012; Detrick et al., 1990; Giger and David, 2017; Hatta and Takeichi, 1986; Pla et al., 2001; Rogers et al., 2013; Scarpa et al., 2015; Schäfer et al., 2014; Shoval et al., 2007). During mesoderm formation of *Drosophila melanogaster*, *Dme*_E-cadherin becomes replaced by *Dme*_N-cadherin (Oda et al., 1998), similar to the switch from E- to N-cadherin during mesoderm formation in chicken (Hatta and Takeichi, 1986). It has also been shown that N-cadherin expression triggers active endodermal cell migration, which leads to cell segregation and germ layer formation (Ninomiya et al., 2012). Moreover, a cadherin switch allows efficient Wnt, bone morphogenetic protein (BMP) and fibroblast growth factor (FGF) signaling, which are required for proper mesoderm differentiation in both the fruit fly and mouse (Basilicata et al., 2016; Giger and David, 2017; Ninomiya et al., 2012; Schäfer et al., 2014). For example, N-cadherin can interact with the FGF receptor and modulate the signaling pathway (Francavilla et al., 2009; Williams et al., 1994). Therefore, accurate control of the expression of cadherins is important for proper cell movements during

[1]Department for Molecular Evolution and Development, Centre of Organismal Systems Biology, University of Vienna, Althanstrasse 14, A-1090 Vienna, Austria. [2]Department of Evolutionary Biology, Biological Faculty, Moscow State University, Leninskie Gory 1/12, 119991 Moscow, Russia.
*Present address: Federal State Budget Institution 'National Medical Research Center for Obstetrics, Gynecology and Perinatology named after Academician V.I. Kulakov of the Ministry of Healthcare of Russian Federation', st. Academician Oparin 4, 117513 Moscow, Russia.

‡Author for correspondence (ulrich.technau@univie.ac.at)

E.A.P., 0000-0001-9498-3084; A.O.K., 0000-0003-4014-4618; Y.A.K., 0000-0003-1916-4200; U.T., 0000-0003-4472-8258

Received 12 December 2018; Accepted 12 September 2019

Development (2019) 146, dev174623. doi:10.1242/dev.174623

gastrulation (e.g. epiboly) and for convergence and extension of the tissue during axis elongation (Babb and Marrs, 2004; Basilicata et al., 2016; Shimizu et al., 2005; Winklbauer, 2012).

Although the role of cadherins has been studied in model bilaterian species, very little is known about their role in diploblastic organisms such as cnidarians. Most of our knowledge on cell adhesion molecules in cnidarians is restricted to genome analyses (Hulpiau and van Roy, 2009, 2011; Tucker and Adams, 2014) or biochemical studies (Clarke et al., 2016). During the last two decades, the sea anemone *Nematostella vectensis* has become one of the prime model organisms for studying embryonic development (Genikhovich and Technau, 2009a; Layden et al., 2016; Technau and Steele, 2011). Bioinformatic analysis of the available genome sequence of *Nematostella vectensis* (Putnam et al., 2007) revealed 16 different cadherins from all main groups of the cadherin superfamily (classical, flamingo, FAT, dachsous, FAT-like, protocadherins and cadherin-related proteins) (Hulpiau and van Roy, 2011). It has been shown that adherens junctions in *Nematostella* ultrastucturally resemble those in bilaterians (Fritzenwanker et al., 2007). However, the molecular composition of these junctions has not yet been described, and a recent report questioned the presence of adherens junctions in the inner layer of *Nematostella* (Salinas-Saavedra et al., 2018).

Germ layers are formed in *Nematostella* by invagination of the endoderm at the animal pole (Kraus and Technau, 2006; Magie et al., 2007). However, whether classical cadherins play a role in germ layer formation in non-bilaterians is not known. Here, we show that the classical cadherins of *Nematostella*, Cadherin 1 (Cdh1) and Cadherin 3 (Cdh3), form the adherens junctions of the epithelium of both germ layers. Germ layer differentiation in *Nematostella* is marked by a cadherin switch, whereby Cdh3 is downregulated in the inner endodermal layer and Cdh1 is upregulated and remains the only cadherin expressed in the endoderm. Unexpectedly, we found that, in addition to apical adherens junctions, both Cdh1 and Cdh3 are involved in cell junctions between cells on the basal-lateral side. Knockdown of *cdh1* and *cdh3* indicated important roles of cadherins in cell adhesion and tissue morphogenesis of this diploblastic metazoan.

RESULTS

Structure of classical cadherins of *Nematostella vectensis*

Three genes encoding classical cadherins have been predicted in the genome of *Nematostella vectensis*, *cadherin1*, *cadherin2* and *cadherin3* (*cdh1*, *cdh2* and *cdh3*) (Hulpiau and van Roy, 2011). However, our analysis of the *cdh2* gene model showed that it is a fusion of two separate gene models for which we have no evidence of its complete transcription; *cdh2* was not detectable by *in situ* hybridization. Furthermore, the hallmarks of the cadherin intracellular domain were absent. Therefore, *cdh2* could either be a pseudogene or the result of incorrect assembly. Hence, this gene model was not investigated further in this study.

Hulpiau and van Roy predicted 25-32 extracellular cadherin (EC) repeats for *Nematostella* cadherins (Hulpiau and van Roy, 2011). However, a more recent publication reported two cadherins with 14 and 30 EC repeats, respectively (Clarke et al., 2016). We cloned both Cdh1 and Cdh2 in overlapping fragments of 2-3 kb length, resulting in full-length cDNA clones of >13 kb, predicting a protein size of about 480 kDa for both cadherins. The protein model suggests a structure similar to classical cadherins, composed of a typical intracellular domain with binding sites for β-catenin and p120, and a large extracellular domain consisting of three EGF-like and two interspaced laminin G (LamG) domains, followed by 30 (Cdh1) or 31 (Cdh3) EC repeats (Fig. 1). This is similar to the original model of Hulpiau and van Roy and we therefore followed their gene terminology. By comparison, fruit fly cadherin has 17 EC repeats, chick cadherin 13 EC repeats and mouse cadherin only 5 EC repeats (Hulpiau and van Roy, 2011).

We also interrogated the genomes and transcriptomes of several other cnidarians and found that all investigated cnidarian cadherins have 30-32 EC domains and the EGF/LamG domains in the extracellular part. Notably, corals and hydrozoans had only a single classical cadherin, whereas the sea anemones underwent a lineage-specific gene duplication (Fig. 1; Fig. S1). Mammals have lost the extracellular EGF and LamG domains and have retained only a few EC domains (Hulpiau and van Roy, 2011). Interestingly, platypus has several paralogs of the short version with no EGF/LamG domains, typical for mammals, but also one classical cadherin with EGF/LamG domains and many EC domains, like other non-mammals. This suggests that an ancestral "long" cadherin gene duplicated in the ancestor of placental mammals and platypus and one of the duplicates underwent a drastic loss of EC and EGF/LamG domains. Platypus has kept both versions, whereas other mammals have retained only duplicates of the short classical cadherin version.

Expression of classical cadherins is highly dynamic during early development of *Nematostella*

To characterize the pattern of classical cadherin expression during normal development, *in situ* hybridization was performed on developmental stages from early cleavage through adult polyp. *cdh3* was maternally expressed at significant levels, detectable at the earliest cleavage stages. *cdh3* was then strongly expressed in all cells from the egg until the gastrula stage (Fig. 2A-D,M). During early gastrulation, *cdh3* expression decreased in the presumptive endoderm (Fig. 2B,C) and was completely downregulated in the endoderm by the planula stage (Fig. 2B-E).

By comparison, *cdh1* expression could not be detected by *in situ* hybridization until the early gastrula stage (Fig. 2G-I), although RNAseq data suggest that it is maternally expressed at lower levels (Casper et al., 2018). During gastrulation, *cdh1* expression first appeared and intensified in the pre-endodermal plate (Fig. 2H,I). At the late gastrula stage, *cdh1* started to be expressed in the aboral ectoderm and then expanded orally during planula development (Fig. 2J,K). Interestingly, at the late planula stage, the strongest *cdh1* expression was detected in the endoderm and in a subpopulation of ectodermal cells, which gave rise to a sensory apical organ (Fig. 2K).

In primary polyps, *cdh3* expression remained strongly expressed in the tentacles and pharynx but weakly in the body-wall ectoderm (Fig. 2F). Interestingly, *cdh3* in juveniles and adults was detectable only in the ectoderm of the pharynx and tentacles, ciliated tract, septal filaments and developing eggs, with hardly any expression in the body-wall ectoderm (Fig. S2A,B). Almost complementary to that, *cdh1* was expressed both in the ectoderm and endoderm, but was completely excluded from the ectoderm of the pharynx and tentacles (Fig. 2L). In juveniles, *cdh1* was expressed in the endoderm and body-wall ectoderm, but not in the ectoderm of most of the pharynx. Interestingly, the part of the pharynx carrying siphonoglyph and the ciliary tract below the pharynx specifically expressed low levels of *cdh1* (Fig. S2C-H). In adults, *cdh1* was expressed in the body-wall endoderm and in small oogonia (Fig. 2N; Fig. S2I).

Development (2019) 146, dev174623. doi:10.1242/dev.174623

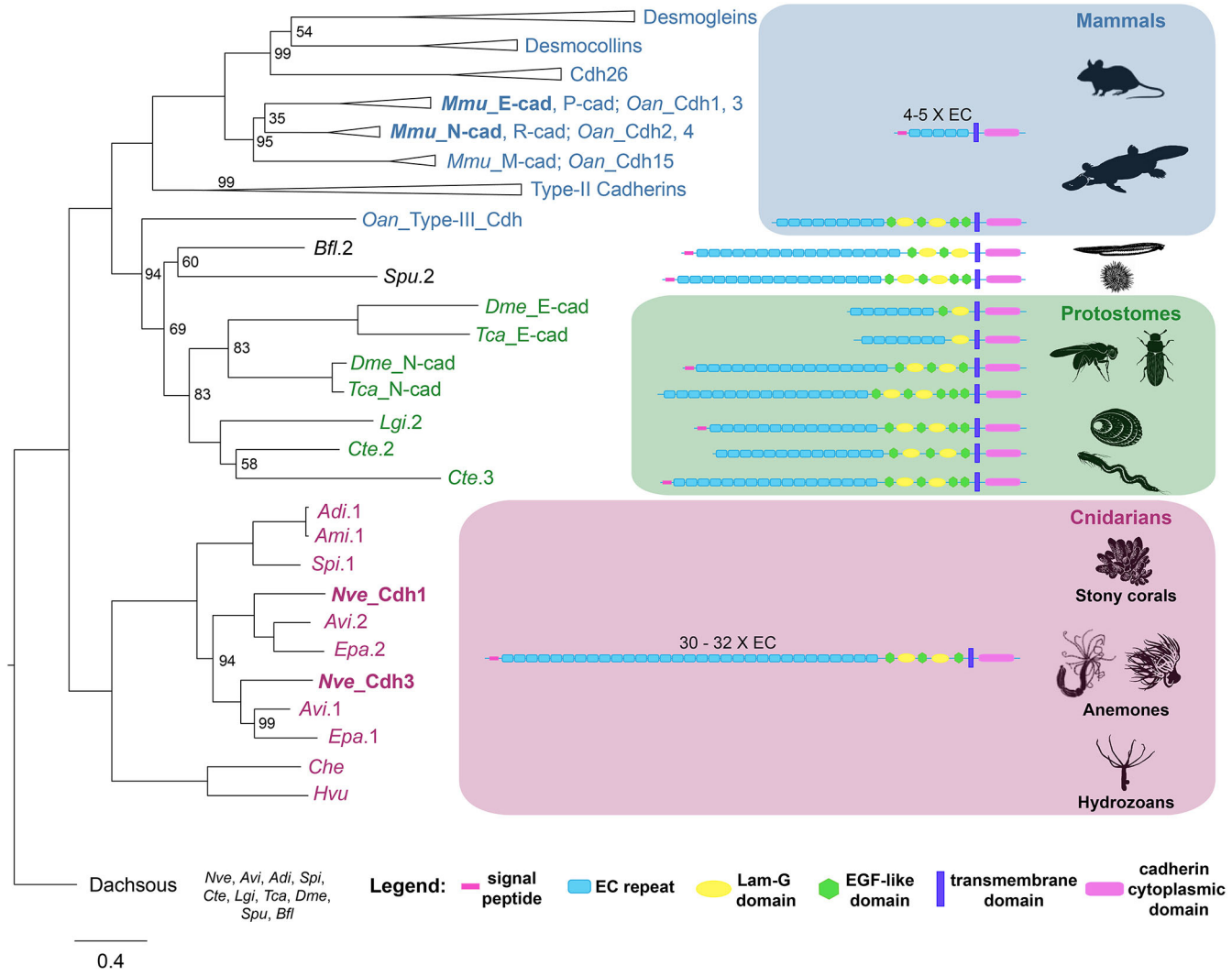

Fig. 1. Maximum likelihood phylogenetic tree of classical and other cadherins. Sequences of all proteins containing a cytoplasmic cadherin domain were extracted from the genomes and transcriptomes of *Mus musculus* (*Mmu*), *Ornithorhynchus anatinus* (*Oan*), *Branchiostoma floridae* (*Bfl*), *Drosophila melanogaster* (*Dme*), *Tribolium castaneum* (*Tca*), *Capitella teleta* (*Cte*), *Lottia gigantea* (*Lgi*), *Nematostella vectensis* (*Nve*), *Anemone viridis* (*Avi*), *Exaiptasia pallida (Epa), Acropora millepora* (*Ami*), *Acropora digitifera* (*Adi*), *Stylophora pistillata* (*Spi*) *Clytia hemisphaerica* (*Che*) and *Hydra vulgaris* (*Hvu*). Proteins with no annotation in their respective databases were assigned an arbitrary number. All gene names are based on the annotations of the respective database, except for *Oan* type-III Cdh, *Nve* Cdh1 and *Nve* Cdh3, which were annotated based on the findings of Hulpiau and van Roy (2011). Dachsous cadherin proteins, which also contain a cytoplasmic cadherin domain, were used as an outgroup. The number at the nodes indicates the bootstrap support; nodes with no label have 100% support. Domain organization is shown on the right. Some proteins lack a signal peptide. This is either an indication of a truncated protein (e.g. *Che*, *Avi*) or a result of assembly mistakes in a gene model.

Cdh3 is the main component of adherens junctions during cleavage and gastrulation

We wished to visualize the subcellular localization of Cdh3 protein during development. We generated specific polyclonal and monoclonal antibodies against two recombinant fragments of Cdh1 and three peptides of Cdh3, respectively (Fig. S3). All antibodies against the different fragments and peptides consistently showed the same pattern for Cdh1 and Cdh3, respectively (Fig. S4) (Madeira et al., 2019). Immunocytochemistry experiments were carried out at all stages of development. Cdh3 protein had already accumulated at the apical cell junctions at the first cell divisions, suggesting a role in establishing early cell polarity. It was also detectable in less confined areas at the lateral contacts between cells (Fig. 3A-C). Interestingly, cells maintained their polarity during cell divisions. In contrast to the Par system proteins (Ragkousi et al., 2017; Salinas-Saavedra et al., 2018), Cdh3 stayed localized at the apical cell junctions at different cell cycle stages (Fig. 4). It is possible that the polarized Cdh3 at the junctions guides the Par system proteins during their transient loss of polarity during cell division. Later, during blastoderm formation, apical cell junctions became more pronounced (Fig. 3D-F). Strikingly, we found that Cdh3 also localized on the basal-lateral side of the cells (Fig. 3D-L), in addition to the apical localization. Ultrastructural analysis by transmission electron microscopy (TEM) revealed that the cell-cell junctions at the basal side resembled the adherens junctions at the apical side (Fig. 3M,N). However, during the blastula stage, asynchronously dividing cells transiently lost the basal-lateral localization of Cdh3 (Fig. 3E, yellow star), similar to the early cleavage stage, when cells divided synchronously (Fig. 3B,C, Fig. 4). Thus, *Nematostella* has a unique epithelium, where cells form cell-cell contacts on both apical and basal sides. These Cdh3-positive junctions developed before any contact to an endodermal

Development (2019) 146, dev174623. doi:10.1242/dev.174623

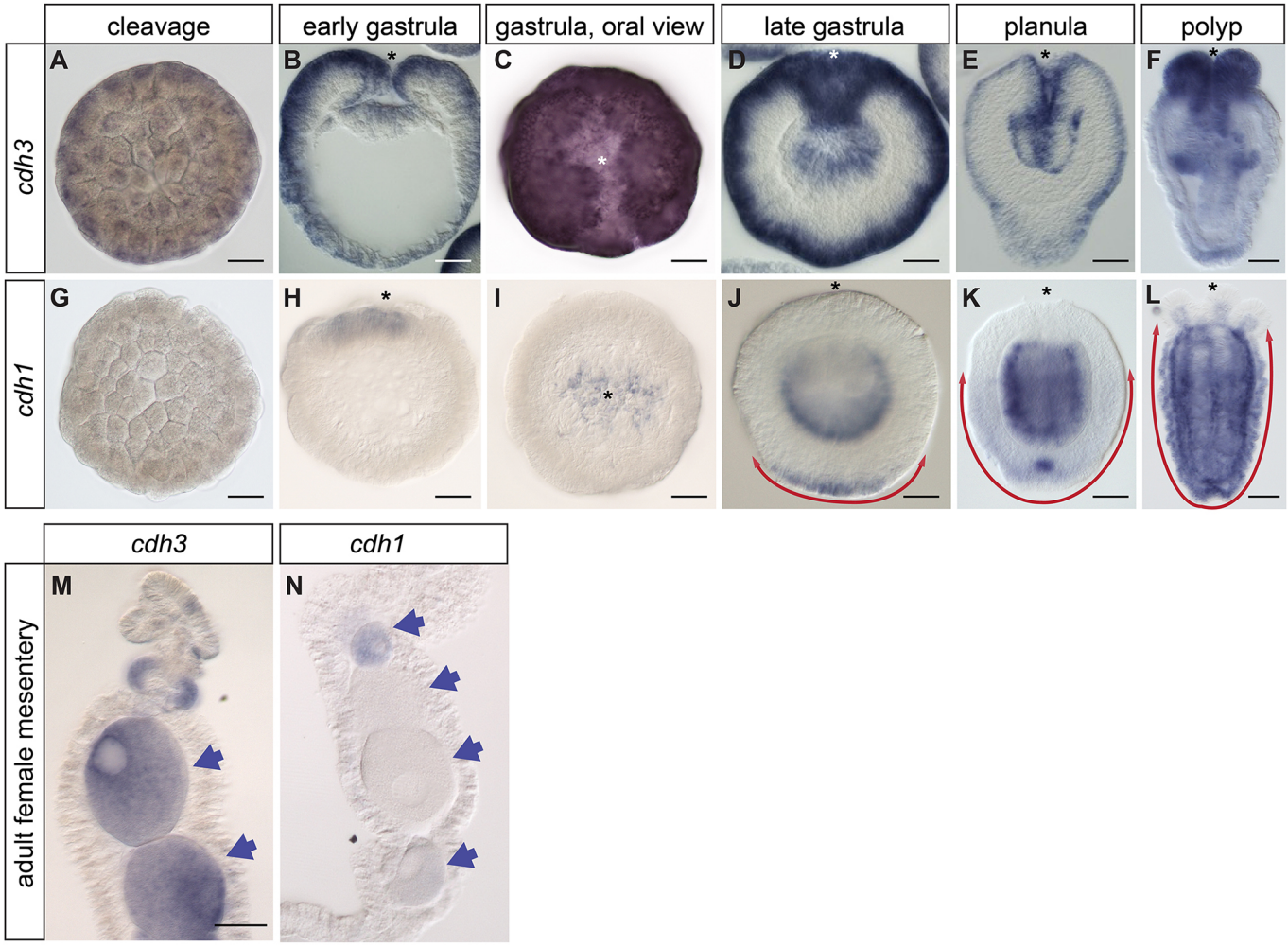

Fig. 2. Expression of *cdh3* and *cdh1* is highly dynamic during early development and polyp growth. (A,G) Cleavage. (B,H) Early gastrula, lateral section. (C,I) Early gastrula, oral view. (D,J) Late gastrula, lateral section. (E,K) Planula, lateral section. (F,L) Primary polyp. (M,N) Adult mesentery section. Double-headed red arrows show expansion of *cdh1* expression on the aboral pole. Arrows indicate the eggs. Asterisk indicates an oral pole. Scale bars: 50 µm in A-L; 100 µm in M,N.

layer or presence of the mesoglea, the extracellular matrix of Cnidaria. This is remarkable and, to our knowledge, has not been described in any other animal. Interestingly, as the pre-endodermal plate began to invaginate and the cells adopted a partial epithelial-to-mesenchymal transition (EMT) phenotype, Cdh3 disappeared from the basal junctions of the invaginating cells (Fig. 3G-I). Meanwhile, ectodermal cells of the blastoderm retained both apical and basal cell contacts. As the pre-endodermal cells lost basal junctions, its epithelium became less rigid and columnar. Pre-endodermal cells formed filopodia and became more motile on the basal side (Fig. 3O). This event is possibly one of the crucial steps of the incomplete EMT, which pre-endodermal cells undergo during gastrulation (Kraus and Technau, 2006; Salinas-Saavedra et al., 2018). Notably, apical cell junctions expressing Cdh3 were preserved in the pre-endodermal cells during the course of gastrulation (Fig. 3J-L).

After the invagination process was complete, Cdh3 fully disappeared from the cell junctions of the endoderm, concordant with the decrease in mRNA expression in the whole endoderm (Fig. 2C-F). Cdh3 remained expressed exclusively in the ectoderm, forming apical and basal cell junctions (Fig. 5A-E). Notably, although the boundary between ectoderm and endoderm is very difficult to discern by morphological criteria, Cdh3 localization at the cell junctions in the pharynx precisely marked the boundary between the last ectodermal cell and the first endodermal cell (Fig. 5B,E). At the polyp stage, Cdh3 remained exclusively expressed in the ectoderm, with especially strong expression in the pharynx and tentacles (Fig. 5F,G).

Cdh1 protein expression marks a cadherin switch during endoderm formation

After completion of gastrulation, Cdh1 protein formed pronounced cellular junctions. In early planula larvae, Cdh1 localized to the apical and basal junctions of the endoderm (Fig. 6A-D). Hence, formation of the endoderm was marked by a cadherin switch from Cdh3 to Cdh1.

It should be noted that the transcriptome data suggested some maternal deposition of *cdh1* in the embryo, even though *in situ* hybridization did not detect *cdh1* until the gastrula stage. Indeed, the anti-Cdh1 antibody detected a fuzzy signal beneath the apical cell membrane in all cells at the early gastrula stage, which might be maternal Cdh1 protein that had not yet localized to the cell junctions.

In addition to endodermal expression, Cdh1 was strongly expressed in the apical organ ectoderm and then expanded into a wider domain in the aboral ectoderm, where Cdh1 and Cdh3 were

Development (2019) 146, dev174623. doi:10.1242/dev.174623

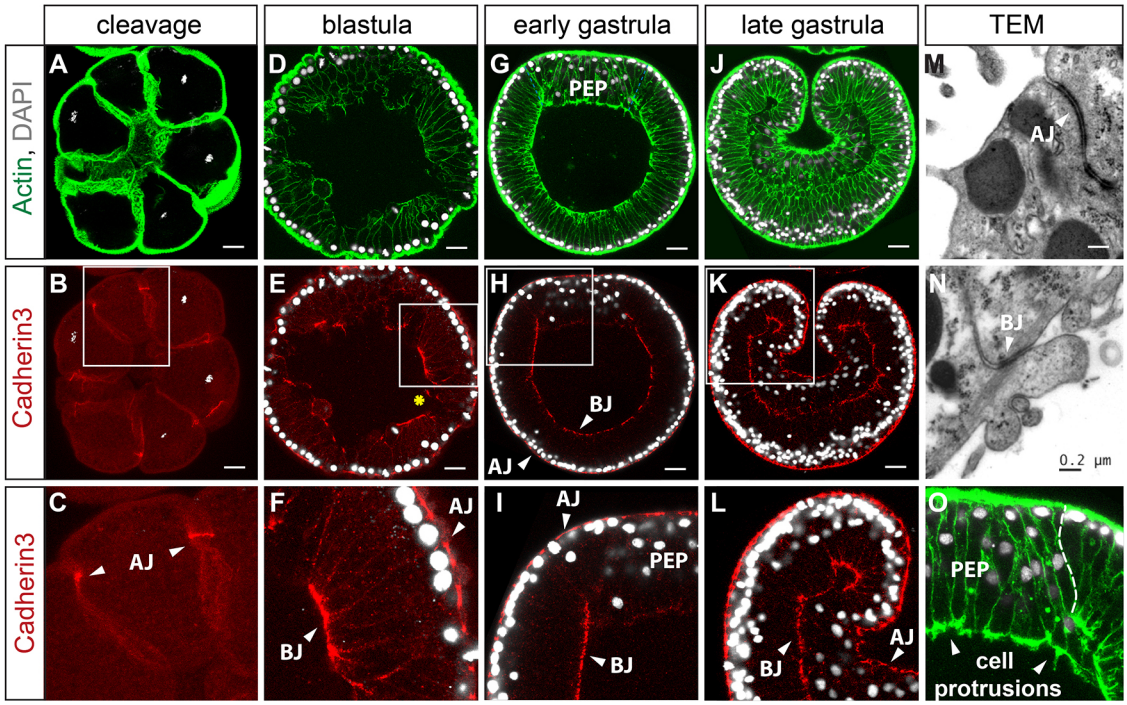

Fig. 3. Cdh3 is a major component of adhesion complexes during cleavage and gastrulation. (A-F) Besides apical junctions (AJ), strong basal epithelial contacts (BJ) form in the blastula during epithelialization. Yellow asterisk is located next to the dividing blastula cell. (G-I) As the pre-endodermal plate (PEP) starts to invaginate, Cdh3 disappears from the BJs and decreases in the AJs in the PEP. Ectodermal cells preserve both apical and basal cell contacts. (J-L) Late gastrula. AJs are present in the ectoderm and in the endoderm. C,F,I,L,O are enlargements of the boxed areas shown in B,E,H,K,G, respectively. (M,N) TEM images of the *Nematostella* epithelium. (O) Cell protrusions on the basal side of the PEP. Scale bars: 20 µm in A,B,D,E,G,H,J,K,O; 0.2 µm in M,N.

co-expressed (Fig. 6). At the ectodermal surface, expression of Cdh1 decreased along a gradient toward the oral pole (Fig. 6L). Interestingly, the ectodermal cell population that gave rise to the apical tuft was also different from the rest of the ectoderm in terms of cadherin expression. These cells lost Cdh3 basal junctions, but kept the apical junctions (Fig. 5C). This specific arrangement might be connected with the special function of these cells (Fig. S5). Indeed, the loss of Cdh3 expression in the ectodermal apical tuft cells went hand-in-hand with upregulation of Cdh1 in these cells (Fig. 2K, Fig. 6A,C).

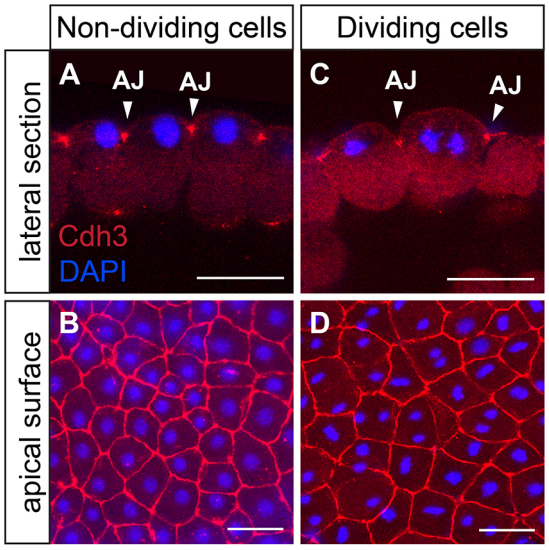

Fig. 4. Cdh3 apical junction localization and cell polarity are preserved during cell division. (A,B) Non-dividing blastula cells. (C,D) Dividing blastula cells at different mitotic phases. AJ, apical junction. Scale bars: 25 µm.

We have demonstrated that Cdh3 is the major component of adhesion complexes during cleavage and gastrulation and is present in all cells until the late gastrula stage. Cdh3 formed apical and basal cell junctions in the blastodermal epithelium, which during invagination of the pre-endodermal plate disappeared from basal cell junctions of the future endoderm. Further endoderm differentiation led to complete Cdh3 to Cdh1 replacement. Therefore, there is a distinct boundary between ectoderm and endoderm, which is defined by the localization of Cdh1 and Cdh3.

Cdh3 in apical ectodermal junctions co-localize with β-catenin

A recent biochemical study showed that the intracellular domain of classical cadherins can form a ternary complex with α-catenin and β-catenin (Clarke et al., 2016). To explore further the molecular composition of the cadherin cell junctions, we co-stained *Nematostella* embryos with the antibody against Cdh3 and with the previously described *Nematostella* antibody against β-catenin (Leclère et al., 2016; Salinas-Saavedra et al., 2018). At blastula stage, Cdh3 was co-localized with β-catenin at the apical junctions, whereas basal junctions did not show such pronounced co-localization (Fig. 7A-C,G-I). Interestingly, at the planula stage, β-catenin was detected only in the body wall ectoderm but not in the ectodermal pharynx nor the endoderm (Fig. 7D-F; Fig. S6). These results could mean that not all the cell contacts of *Nematostella* epithelium contain β-catenin, in line with other recent findings (Salinas-Saavedra et al., 2018). This is surprising, as no ultrastructural differences in the junctions of endoderm and ectoderm could be detected (Fig. S7).

Development (2019) 146, dev174623. doi:10.1242/dev.174623

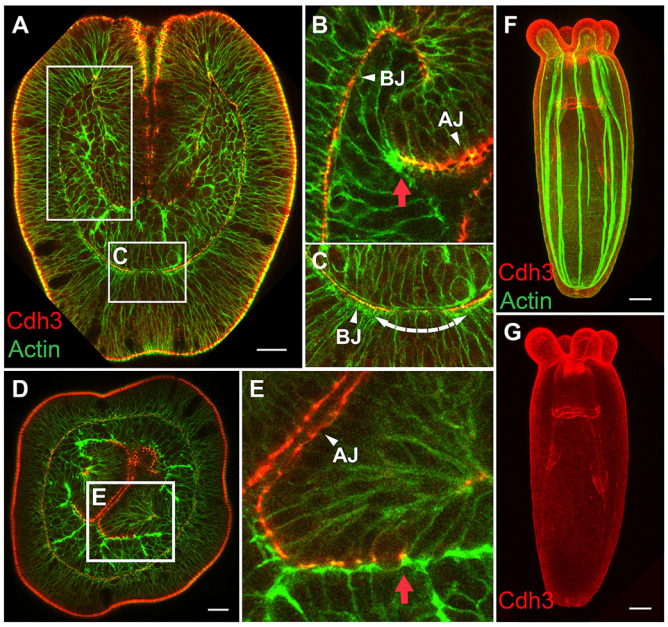

Fig. 5. Cdh3 marks the boundary between ectoderm and endoderm. (A-C) Lateral section of planula. B,C are enlargements of the boxed areas shown in A. (D,E) Cross-section of planula. Ectodermal-endodermal boundary in the pharynx is distinctly labeled by Cdh3 localization in the cell junctions. E is an enlargement of the boxed area shown in D. (F,G) Primary polyp. Cdh3 is expressed exclusively in the ectoderm, forming apical and basal adherens junctions. Red arrow indicates the boundary between the last ectodermal cell and the first endodermal cell. AJ, apical junction; BJ basal junction. Scale bars: 20 µm.

Function of classical cadherins in early development

To examine the function of cadherins, we performed knockdown experiments using morpholinos (MOs) and short hairpin RNA (shRNA). First, we injected independently two non-overlapping translation-blocking *cdh3* MOs. However, we could still detect Cdh3 in apical and basal cell junctions in the whole mount MO-injected embryos (Fig. 8). Indeed, on the ultrastructural level, the adherens cell junctions looked similar in morphants and in control embryos (Fig. 7D,H; Fig. 8C,G). These results can be explained by the significant maternal deposition of mRNA and protein (Figs 2M, 3B). However, development of Cdh3 morphants was arrested after the gastrula stage, presumably due to the block of translation of zygotically expressed *cdh3*. As a result, when Cdh3 protein became limited, post-gastrula embryos were unable to develop further (Fig. 8A,B).

The mild knockdown effect on the presence of Cdh3 in the junctions also suggests that there is relatively little turnover in established junctions. Therefore, to assess the function of Cdh3 in establishing new cell junctions we used an aggregate assay. *Nematostella* gastrulae can be dissociated into single cells and small clusters and can be re-aggregated by centrifugation into cell aggregates (Kirillova et al., 2018). We followed the establishment of cell contacts and the formation of the epithelium in developing cell aggregates (Fig. 9). Dissociated cells did not show any signs of polarization: Cdh3 was not localized to any side (Fig. 9C). Cdh3 became localized to the apical side of the outer cells of the aggregate only 30 min after re-aggregation, and the first signs of epithelialization became apparent (Fig. 9E,F,M). At 12 h after re-aggregation, the outer epithelial layer was completely formed and Cdh3 was localized at the apical and basal cell junctions (Fig. 9H,I). We have previously reported that the two epithelial layers (ectoderm and endoderm) are formed 24 h after re-aggregation (Kirillova et al., 2018). Both cell layers possessed basal and apical cadherin cell junctions (Fig. 9K,L,S). Cdh1 began to be expressed in both ectoderm and endoderm at 24 h of aggregate development (Fig. 9N,Q,T,W). Similar to the normal embryo, the ectoderm expressed both Cdh1 and Cdh3, whereas the endoderm expressed exclusively Cdh1 (Fig. 9U,X).

To address the question of how Cdh3 downregulation influences the establishment of new cell contacts in the aggregate, we dissociated equal amounts of *cdh3* MO-injected gastrulae and standard MO-injected gastrulae (as a control). The first difference we observed was that the size of the aggregates from *cdh3* morphant cells was significantly smaller than control aggregates ($P<0.0001$) (Fig. 10M-O). Moreover, aggregates from *cdh3* MO-injected embryos started to fall apart into cells immediately after re-aggregation (Fig. 10; Movies 1 and 2). Cdh3 knockdown in the aggregate at the protein level was shown by immunostaining (Fig. 10I,J). Ultrastructural imaging with TEM confirmed that cells in Cdh3 MO aggregates did not form well-defined subapical adherens junctions, whereas cell contacts were well developed in the control aggregate (Fig. 10K,L). Interestingly, cells in the Cdh3 MO aggregates made lamella-like protrusions extending to the neighboring cell on the apical surface (Fig. 10K). These results show that *cdh3* knockdown impairs the *de novo* formation of cell contacts, although it does not affect the earlier established contacts built from the maternal protein.

To further explore the role of Cdh1 protein, we downregulated *cdh1* using an independent approach, shRNA-mediated knockdown (He et al., 2018). As in MO knockdown, shRNA knockdown led to a significant decrease in Cdh1 protein, as assayed by immunohistochemistry (Fig. 11; Fig. S8). Although early development (including gastrulation) appeared largely unaffected, mesenteries did not form upon *cdh1* knockdown in the subsequent planula stage. In all MO- and shRNA-injected embryos, mesenteries were absent or impaired, whereas eight mesenteries developed in all control embryos at this stage (Fig. 11, Fig. 12D,H).

In addition to the predominant expression in the endoderm, *cdh1* was also expressed in the apical tuft region of the ectoderm (Fig. 2K). Interestingly, *cdh1* knockdown abolishes expression of FGFa1, which is responsible for apical organ development (Rentzsch et al., 2008). In most *cdh1* MO-injected embryos, the apical organ did not form and there was lack of *FGFa1* expression (Fig. 12). These results suggest that Cdh1 is crucial for morphogenesis and differentiation of the endoderm as well as for development of the apical organ.

DISCUSSION

Evolution and structure of cadherins

Although proteins with cadherin domains are present in choanoflagellates, cadherins with intracellular catenin binding domains are an important class of cell adhesion molecules that arose only in metazoans (Nichols et al., 2012). Cadherins mediate not only cell adhesion between epithelial cells, but are strongly involved in the differentiation of specific cell types. Recently, cadherins have also been shown to convey mechanotransduction (i.e. activation of gene expression in the nucleus in response to mechanical stress), which is mediated by β-catenin in *Drosophila* and *Nematostella* (Iyer et al., 2019; Pukhlyakova et al., 2018; Röper et al., 2018). However, most studies on the role of cadherins have been carried out in bilaterian model organisms such as mouse or *Drosophila*. Here, we show the localization and function of both classical cadherins in a representative of the Cnidaria, the sea anemone *Nematostella vectensis*. Phylogenetic analysis suggests

Development (2019) 146, dev174623. doi:10.1242/dev.174623

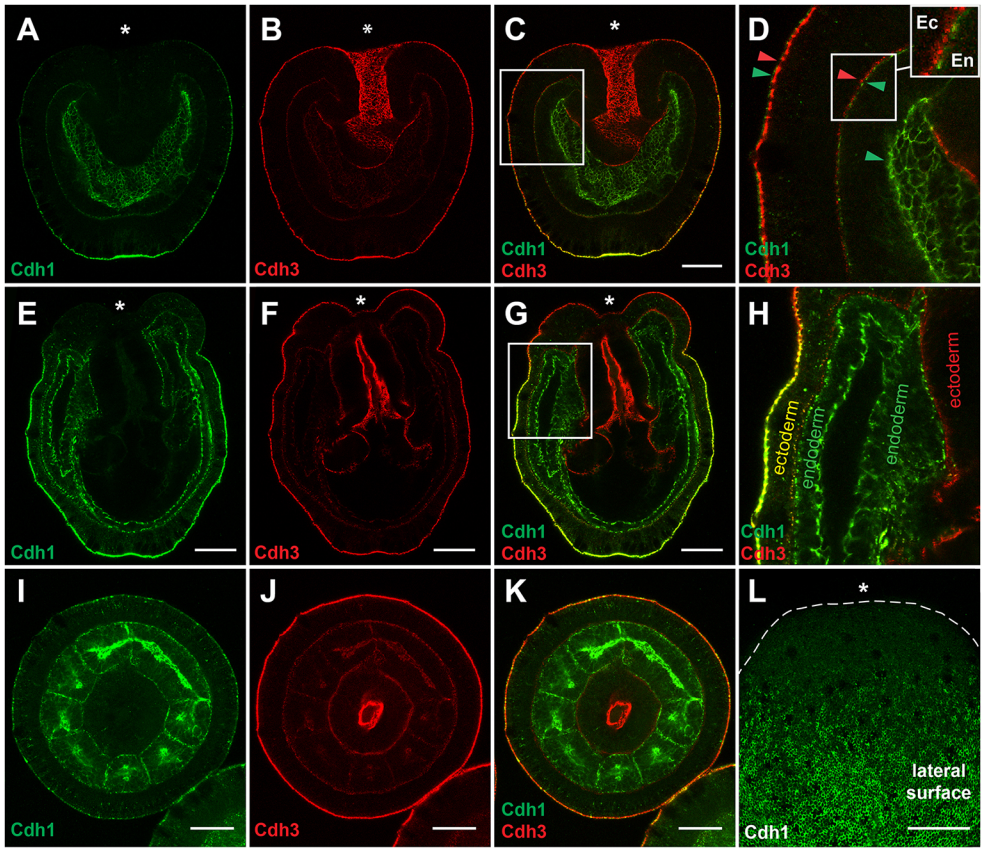

Fig. 6. Cdh1 and Cdh3 localization during germ layer differentiation. (A-D) Planula lateral section. D is an enlargement of the boxed area shown in C. (E-H) Lateral section of the primary polyp. H is an enlargement of the boxed area shown in G. (I-K) Planula cross-section. (L) Surface of the planula; the oral part of the ectoderm is free of Cdh1. Cdh1 is localized in the apical and basal junctions of the endoderm, as well as in the apical junctions and basal junctions of the aboral ectoderm, especially in the area of the apical organ. Cdh1 is gradually disappearing from the ectoderm toward the oral pole and completely excluded from the ectoderm of the tentacles and the pharynx. Cdh3 is localized to the apical and basal junctions of the body wall ectoderm, the ectoderm of the pharynx and is completely excluded from the endoderm. Asterisk marks an oral pole. Scale bars: 50 µm.

that sea anemones have duplicated an ancestral classical cadherin, whereas corals and hydrozoans have retained a single copy. The two investigated cadherin genes code for large proteins with 31-32 EC domains each, largely confirming previous predictions from the genome (Hulpiau and van Roy, 2011) and gene models based on our transcriptome assembly (Fredman et al., 2013). This significantly extends the structure of the recently published gene model for Cdh3 (termed Cad1 in Clarke et al., 2016). Thus, the classical cadherins of cnidarians and other non-bilaterians are substantially larger than those of most bilaterians and their extracellular domain structure is

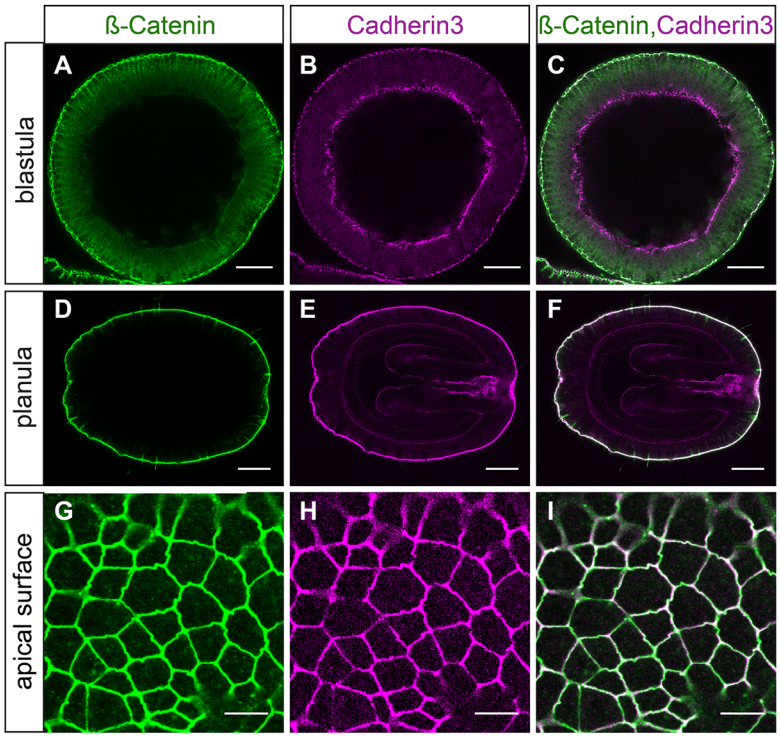

Fig. 7. Cdh3 and β-catenin are co-localized at the apical cell junctions of the ectoderm. (A-C) blastula stage. (D-F) planula stage. (G-I) Apical surface of the ectoderm. Note that only weak β-catenin staining can be detected at the basal ectodermal junction and none in the endoderm. Scale bars: 50 µm in A-F; 10 µm in G-I.

Development (2019) 146, dev174623. doi:10.1242/dev.174623

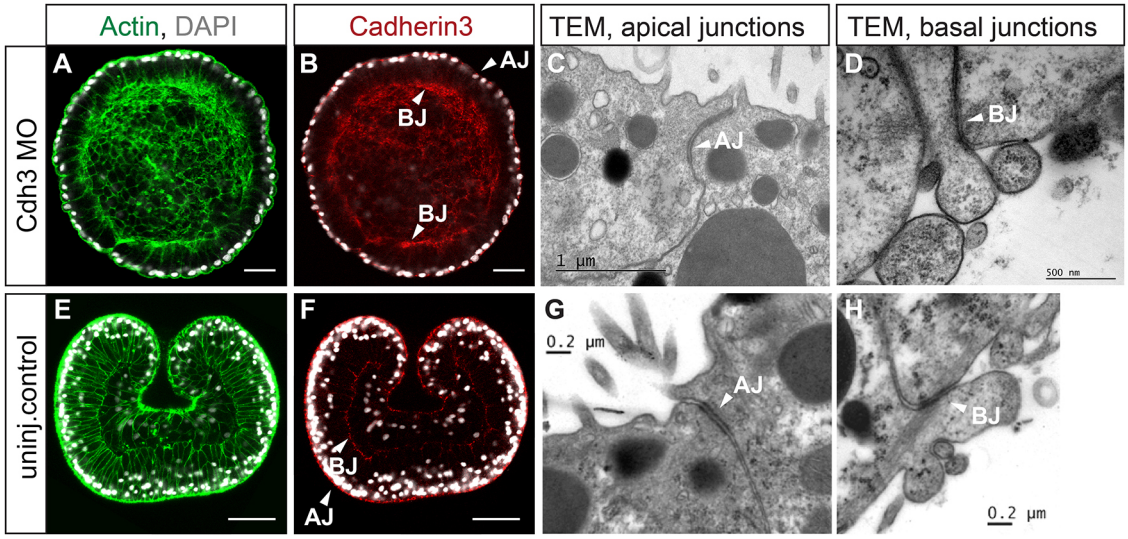

Fig. 8. Cdh3 knockdown blocks gastrulation movements. (A-D) Cdh3 MO-injected embryos at 28 h post-fertilization (hpf). (E-H) Control embryos at 28 hpf. Apical (AJ) and basal (BJ) cell junctions of Cdh3 morphants look very similar to the cell junctions of the control gastrulae. Scale bars: 40 µm in A,B,E.F.

reminiscent of the FAT-like proteins (Hulpiau and van Roy, 2009, 2011). It will be interesting to determine which extracellular domains are engaged in homophilic or heterophilic interactions.

Cadherins are localized to apical and basal junction in both germ layers

Interestingly, both cadherins localized to apical junctions as well as to basal cell-cell junctions in the epithelial cells of both ectoderm and endoderm (Fig. 13A). Electron and confocal microscopy analyses showed actin filaments attached to the junction, suggesting that these are adherens junctions (Fig. 3G,N, Fig. 8D,H). This is in contrast to a recent study claiming that the endodermal epithelium does not contain adherens junctions, since neither Par complex components nor β-catenin could be detected (Salinas-Saavedra et al., 2018). Yet, in line with this study (Salinas-Saavedra et al., 2018), we could detect β-catenin in the apical adherens junctions and weakly in the basal junction of the ectoderm, but not in the pharyngeal ectoderm and the endoderm (Fig. 7; Fig. S6). This could indicate that the basal junctions in the ectoderm and all endodermal junctions are qualitatively different. However, apical adherens junctions in the ectoderm and endoderm have a very similar structure at the ultrastuctural level (Fig. S7). As we observed co-localized actin fibers at these junctions, we assume that another protein replaced β-catenin or that β-catenin was not detected at these junctions. Indeed, we note that the antibody also failed to stain nuclear β-catenin after early cleavage stages. Therefore, as a cautionary note, we cannot fully rule out that the failure to stain β-catenin in the pharynx and the endoderm was due to technical reasons.

To our knowledge, the basal-lateral junctions involving specific cadherins have not yet been described in other animals, but fuzzy basal-lateral localization of cadherins has been observed in other systems. For instance, the midgut epithelium of *Drosophila* shows a basal-lateral localization of a cadherin (Chen et al., 2018), albeit much less defined than described here for *Nematostella*.

Basal junctions might be an innovation of Cnidaria and play a crucial role in morphogenesis of the epithelium. Formation of the basal junctions might be connected to the special properties and functions of the cnidarian epithelium. For example, Hydra epithelia are composed of multifunctional epithelio-muscular cells. These cells form basal myonemes, connected between neighboring cells by desmosomal-like junctions (Seybold et al., 2016). These basal connections could be associated with the contractile actin bundles and used for the increased synchronized contractile activity within large epithelia sheets. Basal cellular contractions also have a major contribution in the process of bud formation in Hydra (Holz et al., 2017). Such basal contacts are absent from bilaterian embryos, which are mainly connected by apical junction belts.

Cadherin and formation of epithelia

Establishment of the adherens junctions is crucial for normal development of the embryo. Knockdown of *cdh3* in normal embryos does not lead to dissociation of embryonic tissue, suggesting that maternally expressed cadherin protein localized in cell junctions might have a slow turnover and be sufficient for the early stages of development. This is consistent with the results of knockdown of E-cadherin in mouse embryos (Capaldo and Macara, 2007). However, proper formation of epithelial layers is disrupted in embryonic aggregates in response to knockdown of *cdh3*. Notably, although knockdown of endodermal *cdh1* does not disrupt gastrulation, the endoderm does not develop endodermal structures such as mesenteries. Thus, proper development of the inner germ layer is dependent on the expression of Cdh1.

The role of cadherins in germ layer formation

The role of cadherins in the formation of germ layers in a diploblast animal is of particular interest, as we might learn about the evolution and potential homology of germ layers. We found that the formation of the inner layer is accompanied by a stepwise cadherin switch. At the blastula stage, Cdh3 forms apical and basal adherens junctions. The onset of gastrulation is characterized by a change in shape of endodermal cells, which adopt a partial EMT phenotype: apical constriction of cells, loss of Cdh3-positive basal junctions, migration of nuclei basally, development of filopodia and an increase in cellular motility (Fig. 13B). We propose that the changes in the adhesion properties of the endodermal cells are crucial for the morphogenetic behavior and further differentiation. In a second step, after completion of invagination, Cdh3 also disappears from the apical junctions in the endoderm and is replaced by Cdh1, both

Development (2019) 146, dev174623. doi:10.1242/dev.174623

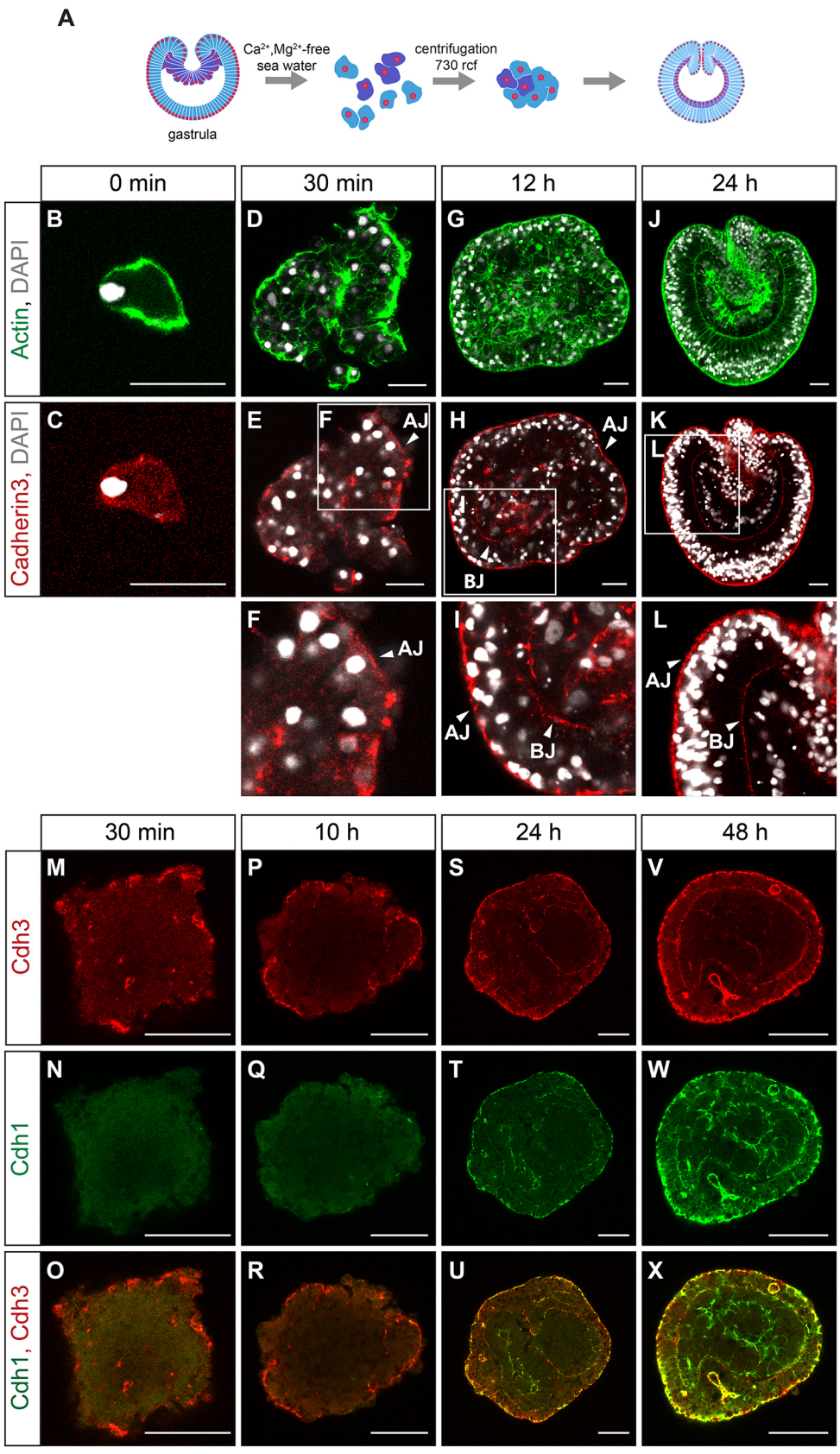

Fig. 9. Reestablishment of polarity and *de novo* formation of the germ layer in the cell aggregate. (A) Scheme of the experiment. (B,C) Dissociated cells do not show polarized Cdh3 localization. (D-F) Epithelialization of the cell aggregate starts ∼30 min after re-aggregation in small groups of cells. (G-I) The ectoderm of the aggregate is fully epithelialized 12 h after dissociation. (J-L) Aggregate has formed two germ layers after 24 h. F,I,L are enlargements of the boxed areas shown in E,H,K, respectively. (M-X) Cdh1 protein appears at the junctions after 24 h of aggregate development. At 48 h after re-aggregation, Cdh1 is broadly expressed in both germ layers. AJ, apical junction; BJ basal junction. Scale bars: 20 µm in B-K; 50 µm in M-X.

at apical and basal junctions of the endoderm. Thus, we observed a cadherin switch in *Nematostella* that is analogous to the cadherin switch in vertebrates and insects. As *cdh1* and *cdh3*, like E- and N-cadherins in mammals and insects, are lineage-specific duplications (Fig. 1), we conclude that the cadherin switch evolved convergently in these animals.

Development (2019) 146, dev174623. doi:10.1242/dev.174623

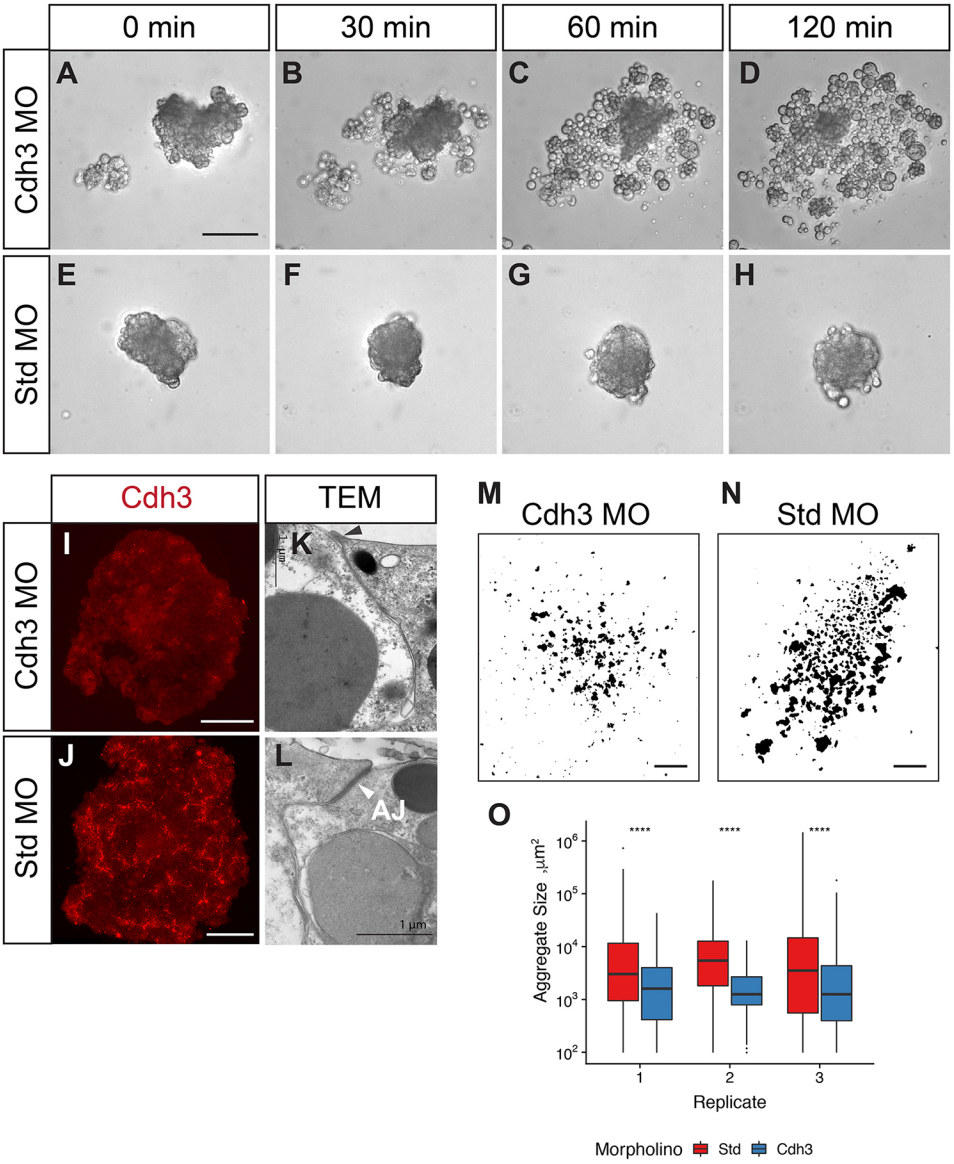

Fig. 10. Cdh3 MO aggregates fail to form adherens junctions *de novo*. (A-D) Cdh3 MO aggregates do not form new cell contacts, fail to develop and fall apart into cells. (E-H) Standard (Std) MO control aggregates stay compact. (I,J) Confocal microscopy images showing downregulation of Cdh3 protein in Cdh3 MO aggregates; Cdh3 antibody staining. (K,L) TEM images of the apical adherens junctions. Apical cell junctions (AJ) of the Cdh3 MO aggregates are much less pronounced than AJs in the control aggregates. (M-O) Cdh3 MO aggregates are significantly smaller than Std MO aggregates. Distribution means within each replicate were tested for significance using a two-sided unpaired Wilcoxon rank-sum test (****P<0.0001). Scale bars: 50 µm in A-J; 1 µm in K,L; 1 mm in M,N.

However, although Cdh3 is not expressed in the endoderm after the gastrula stage, Cdh1 shows partially overlapping expression with Cdh3 in the ectoderm. Cdh1 seems to form a decreasing gradient from aboral to oral, but the significance of this gradient is unclear at this point. Notably, the oral region and tentacles are completely devoid of Cdh1 expression. Interestingly, *cdh1* knockdown does not disrupt oral patterning. For example, expression of the blastopore marker *brachyury* was normal. However, expression of the aboral patterning gene *FGFa1* was abolished (Fig. 12). Because the aboral part is an area of strong Cdh1 expression, we assume that normal Cdh1 expression is necessary for FGF signaling and apical organ development. Our results show that *Nematostella* cadherins are important for germ layer morphogenesis and the maintenance of tissue integrity. However, so far we have no evidence that cadherins play a role in initial germ layer differentiation, as shown similarly for the knockdown of α-catenin, another component of the adhesion junction complex (Clarke et al., 2019). We conclude that, as for bilaterians (Basilicata et al., 2016; Giger and David, 2017; Huang et al., 2016; Nakagawa and Takeichi, 1998; Pla et al., 2001; Schäfer et al., 2014; Shoval et al., 2007), different combinations and concentrations of Cdh1 and Cdh3 convey different tissue properties and identities in different regions of the developing embryo. Thus, the combinatorial and differential use of cadherins is a recurring feature of metazoans (Fig. 1, Fig. 13C; Fig. S1), although the paralogous molecules have evolved independently.

Interestingly, our phylogenetic analysis of the classical cadherins showed that hydrozoans and stony corals have only cadherin protein, which groups basally with two classical cadherins of sea anemones, suggesting that *cdh1* and *cdh3* arose by a lineage-specific gene duplication within the sea anemones (Fig. 1). The expression and function of the single cadherin in other cnidarians is unknown. However, they do have a *dachsous* gene, which also encodes a cytoplasmic cadherin domain and has a similar structure to classical cadherins, except that they lack the EGF/LamG domains found in most invertebrate cadherins. It remains to be shown whether Dachsous and classical cadherin could interact during early germ layer formation in other cnidarians.

Development (2019) 146, dev174623. doi:10.1242/dev.174623

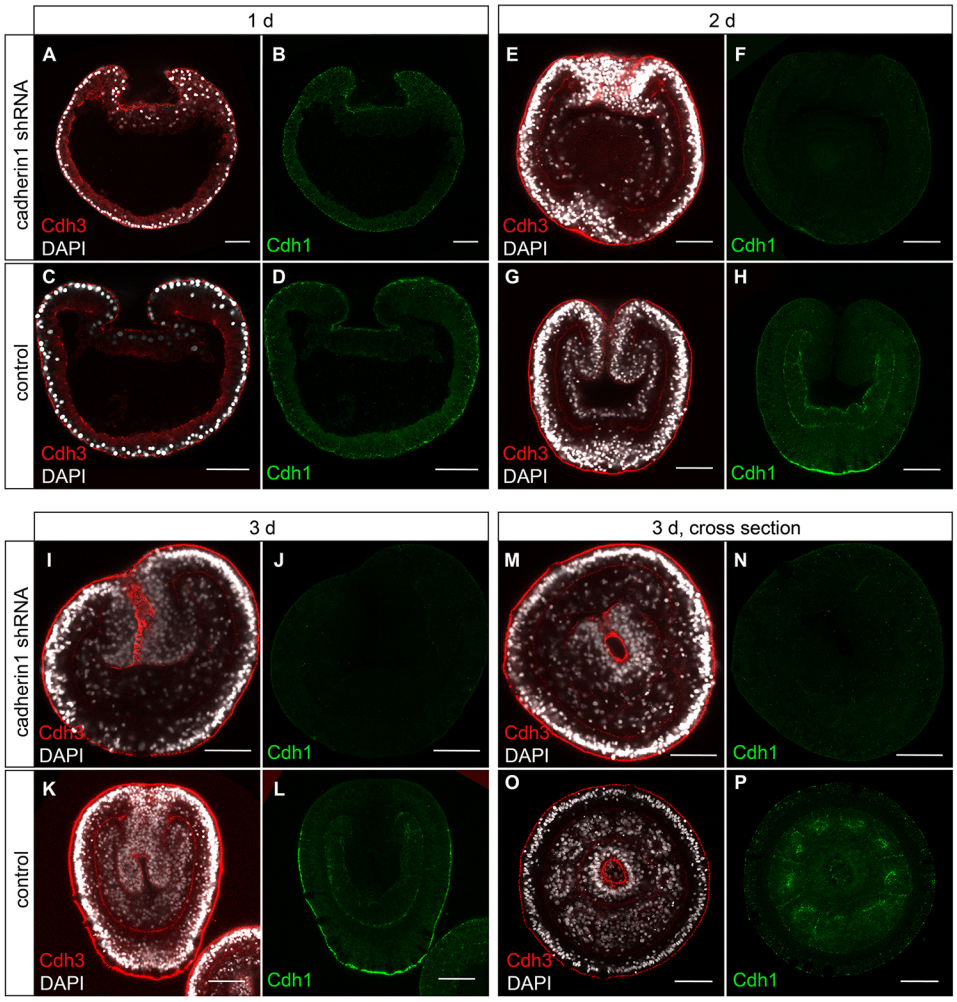

Fig. 11. Mesenteries do not develop after Cdh1 knockdown by shRNA injection. Cdh1 protein expression is strongly downregulated. (A-D) Gastrula stage at 1 day post-fertilization (dpf), lateral section. (E-H) Planula at 2 dpf, lateral section. (I-L) Planula at 3 dpf, lateral section. (M-P) Planula at 3 dpf, cross-section. Scale bars: 50 µm.

Homology of germ layers

Our study has established that cadherins play an important role in the formation and differentiation of the germ layers in a diploblastic animal. This revives the question of which germ layers in Bilateria these two cell layers are homologous with. Traditionally, they have been homologized with the endoderm and ectoderm, with the mesoderm missing. The identification of a number of mesodermal transcription factors in cnidarians and their expression in the endoderm led to the notion of an inner "mesendoderm" (Fritzenwanker et al., 2004; Kumburegama et al., 2011; Martindale, 2004; Salinas-Saavedra et al., 2018; Scholz and Technau, 2003). However, recent analysis of many endodermal and mesodermal marker genes suggests that segregation has already taken place in the *Nematostella* polyp. In fact, the inner layer corresponds to mesoderm, whereas all endodermal functions reside in the ectodermally derived extensions of the pharynx, the septal filaments (Hashimshony, 2017; Steinmetz et al., 2017). In the light of those findings, it is interesting to note that Cdh1 is specific to the inner cell layer, which corresponds to the mesoderm of bilaterians. Notably, this cell layer also expresses the zinc finger transcription factor *snailA* (Fritzenwanker et al., 2004; Martindale, 2004). Snail proteins regulate the downregulation of *E-cadherin* in vertebrates and insects in the ingressing mesoderm (Nieto, 2002). In line with this, *snail* genes appear to play a role in regulating invagination and partial EMT in *Nematostella* (Salinas-Saavedra et al., 2018). It will be of interest to investigate how cadherins are regulated by Snail in *Nematostella*.

Conclusion

This first analysis of the expression and function of classical cadherins in a diploblast shows that these molecules play a conserved role in cell adhesion, tissue morphogenesis and germ layer specification during embryogenesis. Invaginating cells show partial EMT, accompanied by a cadherin switch. The evolutionarily recurring mechanism of a cadherin switch suggests that the evolution of germ layer formation and tissue morphogenesis is facilitated by the differential expression of cadherins.

MATERIALS AND METHODS

Animals and embryo culturing

Animals were kept in artificial seawater at 18°C the dark. Spawning was induced by temperature shift to 24°C and light exposure over 10 h (Fritzenwanker and Technau, 2002). *In vitro* fertilized embryos were collected and kept at 21°C as described (Fritzenwanker and Technau, 2002; Genikhovich and Technau, 2009c).

Identification of Cdh1 and Cdh3 protein sequences

To retrieve the coding sequences of *cdh1* and *cdh3* genes the 1-3 kb overlapping coding fragments of *cdh1* and *cdh3* were amplified from cDNA of mixed embryonic stages, cloned using pJet1.2/blunt vector system (Thermo Fisher Scientific) and sequenced. The full-length sequences of

Development (2019) 146, dev174623. doi:10.1242/dev.174623

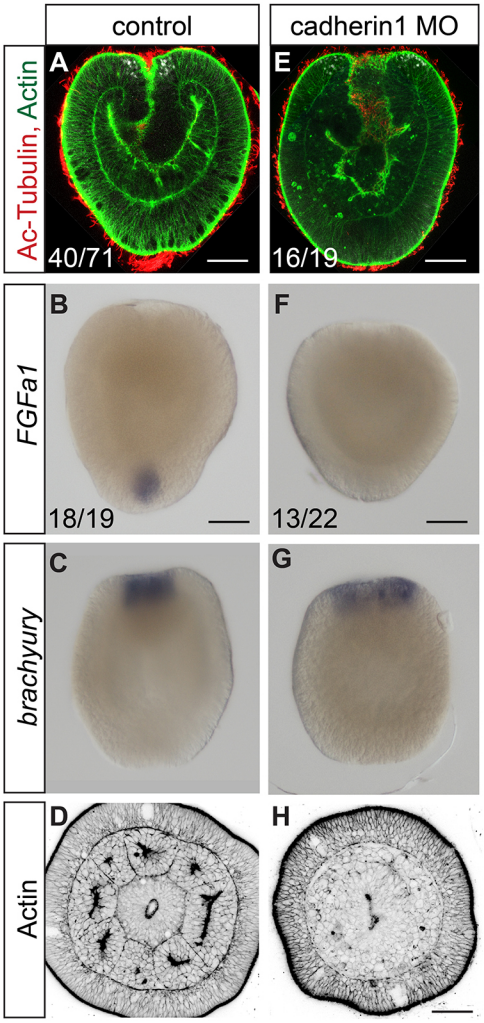

Fig. 12. Cdh1 knockdown impairs apical organ development. (A-D) Control embryo. (E-H) Cdh1 MO knockdown. Apical organs fail to develop (acetylated tubulin antibody staining). *FGFa1* is not expressed. Mesenteries do not form (phalloidin staining). *Brachyury* expression is normal. Scale bars: 50 µm.

Cdh1 and Cdh3 have been deposited in GenBank (accession numbers MK253651 and MK253652).

Assembled *cdh1* and *cdh3* protein coding sequences were derived *in silico* using Expasy translation tool (Artimo et al., 2012). Cadherin protein domain annotation was performed using SMART protein domain annotation resource (Letunic and Bork, 2018).

Morpholino injection

Knockdowns of *cdh1* and *cdh3* were performed by independent zygote injections of two non-overlapping translation blocking morpholinos (Gene Tools): cdh1MO1 5′-CCGGCCAGCACTCATTTTGTGGCTA-3′, cdh1MO2 5′-ACCCGTGAGTTTAAAAACCCATAGC-3′; cdh3MO1 5′-ACGAGTTG-CGGTGAACGAAAATAAC-3′, cdh3MO2 5′-TAGCAGAACCGTCCAGT-CCCATATC-3′ at concentrations of 500 µM. Standard morpholino injection at 500 µM was used as a control; SdtMO 5′-CCTCTTACCTCAGTTACAATT-TATA-3′.

Non-overlapping morpholinos for *cdh1* and *cdh3* knockdown had similar phenotypes.

Injection equipment used: FemtoJet (Eppendorf), CellTram Vario (Eppendorf), micromanipulator (Narishige). Needles were pulled from the glass capillaries type GB 100TF-10 (Science Products) with a micropipette puller (Sutter Instrument, Model P-97). We used holding capillaries from Eppendorf for the injection (Renfer et al., 2010).

Short hairpin RNA knockdown

cdh1 shRNA design and synthesis were performed as described (He et al., 2018). The following primers were used for *cdh1* shRNA synthesis: *cdh1* shRNA forward, 5′-TAATACGACTCACTATAGAAGCGCGCTCAGGT-AAATGTTTCAAGAGA-3′; *cdh1* shRNA reverse, 5′-AAGAAGCACG-TTCGGGTAAATGTTCTCTTGAAACATTTACCTGAGCGC-3′.

Purified shRNA was injected into zygotes at a concentration of 500 ng/µl. As a negative control, shRNA against mOrange was injected at 500 ng/µl. Uninjected embryos from the same batch were used as a control for injection. After injection, embryos were raised at 21°C.

Generation of Cdh1 and Cdh3 antibodies

To generate antibodies against Cdh1, we expressed the protein domains cdh1:domain1 (extracellular) and cdh1:domain3 (intracellular) in *E.coli.* The fragment sequences were as follows: Cdh1 domain1 (extracellular), NAPKDGSLLIIVNAYDGNFTGGVIGKPYYQDDDFDGDENTYELNS-QSPGSYFRVNEGNGDITAAPMIPMGEYNLKIRVTEKKDSPSTVTSS-VRVLVRRIDKEAVDNGVAVEFTDMRKVGYFVGDYYKGFEDVLA-STLGVPTGDIKIFSVQKAHDNGLAVVVFFTVAAKDSYMPHWDVVS-KLVDAKKPLESLGLKVSRLGMD; and Cdh1 domain3 (intracellular), RRPEPVVVYADSTDTGHVHDNVRLYHDDGGGEEDNLGYDITKLM-KYTYIETTIAPPSVAPSKASEDKISTSSDQPLLQGRPPDAVFGLTGK-EPGPKMPKYMEGDDVGDFITTRVKITDREVFLAVDELHIYRYEGDD-TDVD.

The recombinant protein fragments were purified by column-based affinity chromatography and used for immunization. Specifically, the extracellular fragment was used for immunization of two rats (polyclonal Cdh1 antibodies 1 and 2) and the intracellular fragment used for immunization of a rabbit (polyclonal Cdh1 antibody 3). All Cdh1

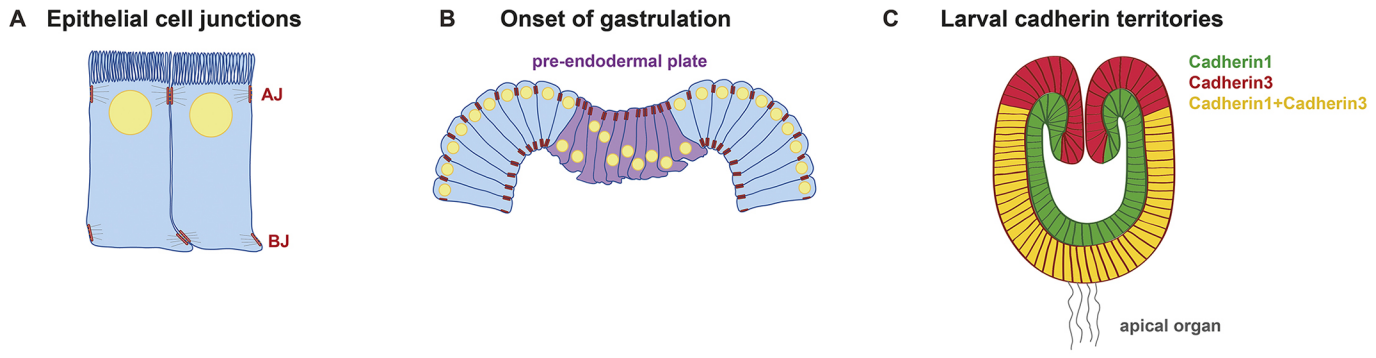

Fig. 13. Cadherin localization during early development of *Nematostella*. (A) Scheme of the apical and basal adherens junctions in both epithelial cell layers. (B) The onset of gastrulation is characterized by downregulation of Cdh3 in the basal junctions, which is accompanied by apical constriction, migration of nuclei to basal positions and formation of filopodia. (C) Overlapping and specific expression domains of Cdh1 and Cdh3 in a planula larva.

Development (2019) 146, dev174623. doi:10.1242/dev.174623

antibodies resulted in the same staining pattern (see Fig. S4). Cdh1 antibody2 was used for most experiments in this paper.

For visualization of Cdh3, monoclonal antibodies were produced in mice. The following peptides were used for immunization: SSSDRNRPPV (for Cdh3 antibody1) and DEKDPPQFSQ (for Cdh3 antibody2). Both epitopes are located in the extracellular part of Cdh3 in the third and seventh cadherin repeats, respectively. Both antibody clones (Cdh3 antibody1 and Cdh3 antibody2) resulted in the same staining patterns (see Fig. S4). Cdh3 antibody2 was used for antibody staining in this paper.

Antibody and phalloidin staining

For Cdh1 antibody staining, embryos were fixed for 1 h at 4°C with Lavdovsky's fixative (3.7% formaldehyde (FA), 50% ethanol, 4% acetic acid). For staining of Cdh3 antibody, β-catenin antibody and phalloidin, embryos were fixed for 1 h with 3.7% FA in PBS at 4°C. Primary polyps were relaxed prior the fixation in 0.1 M $MgCl_2$ in *Nematostella* medium for 10 min. After fixation, embryos were incubated on ice in ice-cold acetone (chilled at −20°C) for 7 min followed by five washes with PBSTx 0.2% (PBS with 0.2% of TritonX-100).

Then embryos were incubated in blocking solution [20% sheep serum, 1% bovine serum albumin (BSA) in PBSTx (0.2%)] for 2 h at room temperature (RT). Primary mouse anti-Cdh3 antibody (1:1000), rabbit β-catenin antibody (1:500; Sigma-Aldrich C2206) (Leclère et al., 2016; Salinas-Saavedra et al., 2018) and/or rat/rabbit anti-Cdh1 antibodies (1:500) were diluted in blocking solution and incubated with the embryos overnight at 4°C, followed by washing in PBSTx 0.2% at RT (10×10 min each). After incubation in blocking solution for 2 h at RT, embryos were placed in a secondary antibody solution of goat anti-mouse Alexa Fluor 568 antibodies (1:1000, Thermo Fischer Scientific A11019), goat anti-rat antibody DyLight 488-conjugated (1:1000, Rockland, 612-141-120) and DAPI overnight at 4°C. When fixed with FA, phalloidin Alexa Fluor 488 (1:30, Thermo Fisher Scientific) was added to the secondary antibody solution, because phalloidin staining is not compatible with the Lavdovsky's fixation. Embryos were washed in PBSTx 0.2% at RT (10×10 min each) and infiltrated with Vectashield antifade mounting medium (Vector laboratories) at 4°C overnight. For β-catenin staining of the embryo sections, fixed embryos were embedded in 10% gelatin in PBS. Gelatin blocks were postfixed in 3.7% FA in PBS overnight at 4°C and sectioned on a vibratome Leica VT 1200S. Embryo sections (50 µm) were stained with β-catenin antibody, phalloidin and DAPI as described for the whole-mount embryos. Imaging was performed with a Leica TCS SP5 DM-6000 confocal microscope.

In situ hybridization

In situ hybridizations of embryos were conducted as previously described (Genikhovich and Technau, 2009b; Kraus et al., 2016). The following regions of the coding sequence of cadherins were used to produce the *in situ* hybridization probes: 7054-9126 bp for *cdh1* and 2728-5091 bp for *cdh3*. Adult animals and juveniles were relaxed for 20 min in 0.1 M $MgCl_2$ solution in *Nematostella* medium followed by fixation and *in situ* hybridization as described (Steinmetz et al., 2017). After *in situ* hybridization embryos, adult and juvenile pieces were embedded in 10% gelatin in PBS. Gelatin blocks were postfixed in 3.7% FA in PBS overnight at 4°C and sectioned on a vibratome Leica VT 1200S. Embryos and adult and juvenile 50 µm sections were embedded in 80% glycerol and imaged with a Nikon Eclipse 80i compound microscope equipped with DIC optics and Zeiss AxioCam camera.

Time-lapse microscopy

Time-lapse imaging was carried out using a Nikon Eclipse 80i compound microscope. Pictures were taken with a Zeiss AxioCam camera. Time-lapse movies were made using FIJI software (Schindelin et al., 2012).

Transmission electron microscopy

Transmission electron microscopy was performed as previously described (Fritzenwanker et al., 2007).

Phylogenetic analysis

The protein complements of *Mus musculus* (GRCm38) (Schneider et al., 2017) and *Drosophila melanogaster* (FB2018_03) (Thurmond et al., 2019) were downloaded from Ensembl (Zerbino et al., 2018); *Strongylocentrotus purpuratus*, *Capitella teleta*, *Lottia gigantica* and *Tribolium castaneum* from Ensembl metazoan (Kersey et al., 2018); *Hydra vulgaris* and *Ornithorhynchus anatinus* from RefSeq at NCBI (O'Leary et al., 2016); *Acropora millepora* (PRJNA74409) (Moya et al., 2012), *Anemonia viridis* (PRJNA260824) (Rachamim et al., 2015), *Exaptasia pallida* (PRJNA386175) (Baumgarten et al., 2015) and *Stylophora pistilata* (PRJNA281535) (Voolstra et al., 2017) from the Sequence Read Archive at NCBI (Leinonen et al., 2011); and *Acropora digitifera* from marine genomics at OIST (Shinzato et al., 2011). Sequences were selected that had a significant domain hit (domE<1×10^{-5}) to the cadherin cytoplasmic Pfam family (PF01049) according to HMMER 3.2.1 (Finn et al., 2011). When multiple isoforms were present, the longest one was used. The genes were filtered against truncated and misassembled gene models manually. Sequences were aligned using MAFFT v7.307 in E-INS-i mode and a maximum of 1000 iterations of refinement (Katoh and Standley, 2013). The WAG+F+R6 model was determined as optimal by the Bayesian Information Criterion using ModelFinder (Kalyaanamoorthy et al., 2017). This was used to infer a maximum likelihood tree using IQTREE (Nguyen et al., 2015). Support values were determined with 1000 standard bootstrap replicates. Domain architectures were determined using standalone interproscan (Mitchell et al., 2019).

Analysis of the size of the cell aggregates

Cdh3 morpholino (MO) embryos and standard MO control embryos (50 of each) were dissociated into cells at the gastrula stage. Cell aggregates were generated by slow centrifugation as described (Kirillova et al., 2018) and photographed immediately after centrifugation. The size of the aggregates was analyzed with FIJI software. (FIJI/Image/Adjust/Threshold tool and FIJI/Analyze/Analyze particles). The threshold was set to 50. The experiment was repeated three times.

Image processing

Images were processed and adjusted for brightness and contrast using FIJI software (Schindelin et al., 2012). Focus stacking of ISH images was done using Helicon Focus software (Helicon Soft, Kharkov, Ukraine). Images were cropped and assembled into the figures; schemes were made using Adobe Illustrator CS6 software (Adobe, San Jose, USA).

Acknowledgements

We thank Eduard Renfer and Sarah Streinzer for cloning the cDNAs for the *in situ* probes of *cdh1* and *cdh3*, and for performing initial *in situ* hybridizations of these genes. We are very grateful to Prof. Bert Hobmayer for the fruitful discussions and to Dr Alison Cole for critical reading of the manuscript. We thank Rohit Dnyansagar for help with generating the phylogenetic tree and Boris Osadchenko for imaging some of the transmission electron microscopy samples. We thank Vienna Biocenter Facilities (VBCF) for support with recombinant cadherin protein generation and purification, and the Core Facility for Cell Imaging and Ultrastructure Research of the University of Vienna (CIUS) for assistance.

Competing interests

The authors declare no competing or financial interests.

Author contributions

Conceptualization: E.A.P., U.T.; Methodology: E.A.P., A.O.K., Y.A.K., B.Z.; Investigation: E.A.P.; Data curation: B.Z.; Writing - original draft: E.A.P., U.T.; Writing - review & editing: E.A.P., U.T.; Supervision: U.T.; Project administration: U.T.; Funding acquisition: U.T.

Funding

This work was funded by an Austrian Science Fund (FWF) grant to U.T. (P25993).

Data availability

Sequences, the alignment file and the suptree file are available at https://doi.org/10.6084/m9.figshare.9919130.v1.

Supplementary information

Supplementary information available online at http://dev.biologists.org/lookup/doi/10.1242/dev.174623.supplemental

References

Alberts, B. (2007). *Molecular Biology of the Cell*. New York: Garland Science.

Angst, B. D., Marcozzi, C. and Magee, A. I. (2001). The cadherin superfamily: diversity in form and function. *J. Cell Sci.* **114**, 629-641.

Artimo, P., Jonnalagedda, M., Arnold, K., Baratin, D., Csardi, G., de Castro, E., Duvaud, S., Flegel, V., Fortier, A., Gasteiger, E. et al. (2012). ExPASy: SIB bioinformatics resource portal. *Nucleic Acids Res.* **40**, 597-603. doi:10.1093/nar/gks400

Babb, S. G. and Marrs, J. A. (2004). E-cadherin regulates cell movements and tissue formation in early zebrafish embryos. *Dev. Dyn.* **230**, 263-277. doi:10.1002/dvdy.20057

Basilicata, M. F., Frank, M., Solter, D., Brabletz, T. and Stemmler, M. P. (2016). Inappropriate cadherin switching in the mouse epiblast compromises proper signaling between the epiblast and the extraembryonic ectoderm during gastrulation. *Sci. Rep.* **6**, 8263. doi:10.1038/srep26562

Baumgarten, S., Simakov, O., Esherick, L. Y., Liew, Y. J., Lehnert, E. M., Michell, C. T., Li, Y., Hambleton, E. A., Guse, A., Oates, M. E. et al. (2015). The genome of Aiptasia, a sea anemone model for coral symbiosis. *Proc. Natl. Acad. Sci. USA* **112**, 11893-11898. doi:10.1073/pnas.1513318112

Capaldo, C. T. and Macara, I. G. (2007). Depletion of E-cadherin disrupts establishment but not maintenance of cell junctions in Madin-Darby canine kidney epithelial cells. *Mol. Biol. Cell* **18**, 189-200. doi:10.1091/mbc.e06-05-0471

Casper, J., Zweig, A. S., Villarreal, C., Tyner, C., Speir, M. L., Rosenbloom, K. R., Raney, B. J., Lee, C. M., Lee, B. T., Karolchik, D. et al. (2018). The UCSC genome browser database: 2018 update. *Nucleic Acids Res.* **46**, 762-769. doi:10.1093/nar/gkv1275

Chen, J., Sayadian, A.-C., Lowe, N., Lovegrove, H. E. and St Johnston, D. (2018). An alternative mode of epithelial polarity in the Drosophila midgut. *PLoS Biol.* **16**, e3000041. doi:10.1371/journal.pbio.3000041

Clarke, D. N., Miller, P. W., Lowe, C. J., Weis, W. I. and Nelson, W. J. (2016). Characterization of the cadherin-catenin complex of the sea anemone *Nematostella vectensis* and Implications for the evolution of metazoan cell-cell adhesion. *Mol. Biol. Evol.* **33**, 2016-2029. doi:10.1093/molbev/msw084

Clarke, D. N., Lowe, C. J. and James Nelson, W. (2019). The cadherin-catenin complex is necessary for cell adhesion and embryogenesis in Nematostella vectensis. *Dev. Biol.* **447**, 170-181. doi:10.1016/j.ydbio.2019.01.007

Dady, A., Blavet, C. and Duband, J.-L. (2012). Timing and kinetics of E- to N-cadherin switch during neurulation in the avian embryo. *Dev. Dyn.* **241**, 1333-1349. doi:10.1002/dvdy.23813

Detrick, R. J., Dickey, D. and Kintner, C. R. (1990). The effects of N-cadherin misexpression on morphogenesis in Xenopus embryos. *Neuron* **4**, 493-506. doi:10.1016/0896-6273(90)90108-R

Finn, R. D., Clements, J. and Eddy, S. R. (2011). HMMER web server: interactive sequence similarity searching. *Nucleic Acids Res.* **39**, W29-W37. doi:10.1093/nar/gkr367

Francavilla, C., Cattaneo, P., Berezin, V., Bock, E., Ami, D., de Marco, A., Christofori, G. and Cavallaro, U. (2009). The binding of NCAM to FGFR1 induces a specific cellular response mediated by receptor trafficking. *J. Cell. Biol.* **187**, 1101-1116. doi:10.1083/jcb.200903030

Fredman, D., Schwaiger, M., Rentzsch, F. and Technau, U. (2013). *Nematostella vectensis* transcriptome and gene models v2.0. *figshare*. https://doi.org/10.6084/M9.FIGSHARE.807696.

Fritzenwanker, J. H. and Technau, U. (2002). Induction of gametogenesis in the basal cnidarian *Nematostella vectensis* (Anthozoa). *Dev. Genes Evol.* **212**, 99-103. doi:10.1007/s00427-002-0214-7

Fritzenwanker, J. H., Saina, M. and Technau, U. (2004). Analysis of forkhead and snail expression reveals epithelial–mesenchymal transitions during embryonic and larval development of *Nematostella vectensis*. *Dev. Biol.* **275**, 389-402. doi:10.1016/j.ydbio.2004.08.014

Fritzenwanker, J. H., Genikhovich, G., Kraus, Y. and Technau, U. (2007). Early development and axis specification in the sea anemone *Nematostella vectensis*. *Dev. Biol.* **310**, 264-279. doi:10.1016/j.ydbio.2007.07.029

Genikhovich, G. and Technau, U. (2009a). The Starlet sea anemone *Nematostella vectensis*: an anthozoan model organism for studies in comparative genomics and functional evolutionary developmental biology. *Cold Spring Harb. Prot.* **2009**, pdb.emo129. doi:10.1101/pdb.emo129

Genikhovich, G. and Technau, U. (2009b). *In situ* hybridization of Starlet sea anemone (*Nematostella vectensis*) embryos, larvae, and polyps. *Cold Spring Harb. Prot.* **2009**, prot5282. doi:10.1101/pdb.prot5282

Genikhovich, G. and Technau, U. (2009c). Induction of spawning in the starlet sea anemone *Nematostella vectensis*, in vitro fertilization of gametes, and dejellying of zygotes. *Cold Spring Harb. Prot.* **4**, prot5281. doi:10.1101/pdb.prot5281

Giger, F. A. and David, N. B. (2017). Endodermal germ-layer formation through active actin-driven migration triggered by N-cadherin. *Proc. Natl. Acad. Sci. USA* **114**, 10143-10148. doi:10.1073/pnas.1708116114

Gilbert, S. F. (2013). *Developmental Biology*. MA: Sinauer Associates, Inc., Sunderland.

Gumbiner, B. M. (2005). Regulation of cadherin-mediated adhesion in morphogenesis. *Nat. Rev. Mol. Cell Biol.* **6**, 622-634. doi:10.1038/nrm1699

Halbleib, J. M. and Nelson, W. J. (2006). Cadherins in development: cell adhesion, sorting, and tissue morphogenesis. *Genes Dev.* **20**, 3199-3214. doi:10.1101/gad.1486806

Hashimshony, T. (2017). Cnidarians layer up. *Nat. Ecol. Evol.* **1**, 1429-1430. doi:10.1038/s41559-017-0323-3

Hatta, K. and Takeichi, M. (1986). Expression of N-cadherin adhesion molecules associated with early morphogenetic events in chick development. *Nature* **320**, 447-449. doi:10.1038/320447a0

He, S., Del Viso, F., Chen, C.-Y., Ikmi, A., Kroesen, A. E. and Gibson, M. C. (2018). An axial Hox code controls tissue segmentation and body patterning in *Nematostella vectensis*. *Science* **361**, 1377-1380. doi:10.1126/science.aar8384

Holz, O., Apel, D., Steinmetz, P., Lange, E., Hopfenmüller, S., Ohler, K., Sudhop, S. and Hassel, M. (2017). Bud detachment in hydra requires activation of fibroblast growth factor receptor and a Rho-ROCK-myosin II signaling pathway to ensure formation of a basal constriction. *Dev. Dyn.* **246**, 502-516. doi:10.1002/dvdy.24508

Huang, C., Kratzer, M.-C., Wedlich, D. and Kashef, J. (2016). E-cadherin is required for cranial neural crest migration in Xenopus laevis. *Dev. Biol.* **411**, 159-171. doi:10.1016/j.ydbio.2016.02.007

Hulpiau, P. and van Roy, F. (2009). Molecular evolution of the cadherin superfamily. *Int. J. Biochem. Cell Biol.* **41**, 349-369. doi:10.1016/j.biocel.2008.09.027

Hulpiau, P. and van Roy, F. (2011). New insights into the evolution of metazoan cadherins. *Mol. Biol. Evol.* **28**, 647-657. doi:10.1093/molbev/msq233

Iyer, K. V., Piscitello-Gómez, R., Paijmans, J., Jülicher, F. and Eaton, S. (2019). Epithelial viscoelasticity is regulated by mechanosensitive E-cadherin turnover. *Curr. Biol.* **29**, 578-591.e5. doi:10.1016/j.cub.2019.01.021

Kalyaanamoorthy, S., Minh, B. Q., Wong, T. K. F., von Haeseler, A. and Jermiin, L. S. (2017). ModelFinder: fast model selection for accurate phylogenetic estimates. *Nat. Meth.* **14**, 587-589. doi:10.1038/nmeth.4285

Katoh, K. and Standley, D. M. (2013). MAFFT multiple sequence alignment software version 7: improvements in performance and usability. *Mol. Biol. Evol.* **30**, 772-780. doi:10.1093/molbev/mst010

Kersey, P. J., Allen, J. E., Allot, A., Barba, M., Boddu, S., Bolt, B. J., Carvalho-Silva, D., Christensen, M., Davis, P., Grabmueller, C. et al. (2018). Ensembl Genomes 2018: an integrated omics infrastructure for non-vertebrate species. *Nucleic Acids Res.* **46**, D802-D808. doi:10.1093/nar/gkx1011

Kirillova, A., Genikhovich, G., Pukhlyakova, E., Demilly, A., Kraus, Y. and Technau, U. (2018). Germ-layer commitment and axis formation in sea anemone embryonic cell aggregates. *Proc. Natl. Acad. Sci. USA* **115**, 1813-1818. doi:10.1073/pnas.1711516115

Kraus, Y. and Technau, U. (2006). Gastrulation in the sea anemone Nematostella vectensis occurs by invagination and immigration: an ultrastructural study. *Dev. Genes Evol.* **216**, 119-132. doi:10.1007/s00427-005-0038-3

Kraus, Y., Aman, A., Technau, U. and Genikhovich, G. (2016). Pre-bilaterian origin of the blastoporal axial organizer. *Nat. Commun.* **7**, 11694. doi:10.1038/ncomms11694

Kumburegama, S., Wijesena, N., Xu, R. and Wikramanayake, A. H. (2011). Strabismus-mediated primary archenteron invagination is uncoupled from Wnt/b-catenin- dependent endoderm cell fate specification in *Nematostella vectensis* (Anthozoa, Cnidaria): Implications for the evolution of gastrulation. *EvoDevo* **2**, 2. doi:10.1186/2041-9139-2-2

Layden, M. J., Rentzsch, F. and Röttinger, E. (2016). The rise of the starlet sea anemone Nematostella vectensis as a model system to investigate development and regeneration. *Wiley Interdiscip. Rev. Dev. Biol.* **5**, 408-428. doi:10.1002/wdev.222

Leclère, L., Bause, M., Sinigaglia, C., Steger, J. and Rentzsch, F. (2016). Development of the aboral domain in *Nematostella* requires β-catenin and the opposing activities of Six3/6 and Frizzled5/8. *Development* **143**, 1766-1777. doi:10.1242/dev.120931

Leinonen, R., Sugawara, H., Shumway, M. and **International Nucleotide Sequence Database Collaboration**. (2011). The sequence read archive. *Nucleic Acids Res.* **39**, 19-21. doi:10.1093/nar/gkq1019

Letunic, I. and Bork, P. (2018). 20 years of the SMART protein domain annotation resource. *Nucleic Acids Res.* **46**, D493-D496. doi:10.1093/nar/gkx922

Madeira, F., Park, Y. M., Lee, J., Buso, N., Gur, T., Madhusoodanan, N., Basutkar, P., Tivey, A. R. N., Potter, S. C., Finn, R. D. et al. (2019). The EMBL-EBI search and sequence analysis tools APIs in 2019. *Nucleic Acids Res.* **47**, W636-W641. doi:10.1093/nar/gkz268

Magie, C. R., Daly, M. and Martindale, M. Q. (2007). Gastrulation in the cnidarian *Nematostella vectensis* occurs via invagination not ingression. *Dev.Biol.* **305**, 483-497. doi:10.1016/j.ydbio.2007.02.044

Martindale, M. Q. (2004). Investigating the origins of triploblasty: 'mesodermal' gene expression in a diploblastic animal, the sea anemone *Nematostella vectensis* (phylum, Cnidaria; class, Anthozoa). *Development* **131**, 2463-2474. doi:10.1242/dev.01119

Meng, W. and Takeichi, M. (2009). Adherens junction: molecular architecture and regulation. *Cold Spring Harb. Perspec. Biol.* **1**, a002899-a002899. doi:10.1101/cshperspect.a002899

Mitchell, A. L., Attwood, T. K., Babbitt, P. C., Blum, M., Bork, P., Bridge, A., Brown, S. D., Chang, H.-Y., El-Gebali, S., Fraser, M. I. et al. (2019). InterPro in 2019: improving coverage, classification and access to protein sequence annotations. *Nucleic Acids Res.* **47**, D351-D360. doi:10.1093/nar/gky1100

Moya, A., Huisman, L., Ball, E. E., Hayward, D. C., Grasso, L. C., Chua, C. M., Woo, H. N., Gattuso, J.-P., Forêt, S. and Miller, D. J. (2012). Whole transcriptome analysis of the coral Acropora millepora reveals complex responses to CO?-driven acidification during the initiation of calcification. *Mol. Ecol.* **21**, 2440-2454. doi:10.1111/j.1365-294X.2012.05554.x

Nakagawa, S. and Takeichi, M. (1998). Neural crest emigration from the neural tube depends on regulated cadherin expression. *Development* **125**, 2963-2971.

Nandadasa, S., Tao, Q., Menon, N. R., Heasman, J. and Wylie, C. (2009). N- and E-cadherins in Xenopus are specifically required in the neural and non-neural ectoderm, respectively, for F-actin assembly and morphogenetic movements. *Development* **136**, 1327-1338. doi:10.1242/dev.031203

Nguyen, L.-T., Schmidt, H. A., von Haeseler, A. and Minh, B. Q. (2015). IQ-TREE: a fast and effective stochastic algorithm for estimating maximum-likelihood phylogenies. *Mol. Biol. Evol.* **32**, 268-274. doi:10.1093/molbev/msu300

Nichols, S. A., Roberts, B. W., Richter, D. J., Fairclough, S. R. and King, N. (2012). Origin of metazoan cadherin diversity and the antiquity of the classical cadherin/β-catenin complex. *Proc. Natl. Acad. Sci. USA* **109**, 13046-13051. doi:10.1073/pnas.1120685109

Nieto, M. A. (2002). The Snail superfamily of zinc-finger transcription factors. *Nat. Rev. Mol. Cell Biol.* **3**, 155-166. doi:10.1038/nrm757

Ninomiya, H., David, R., Damm, E. W., Fagotto, F., Niessen, C. M. and Winklbauer, R. (2012). Cadherin-dependent differential cell adhesion in Xenopus causes cell sorting in vitro but not in the embryo. *J. Cell Sci.* **125**, 1877-1883. doi:10.1242/jcs.095315

Oda, H. and Takeichi, M. (2011). Structural and functional diversity of cadherin at the adherens junction. *J. Cell Biol.* **193**, 1137-1146. doi:10.1083/jcb.201008173

Oda, H., Tsukita, S. and Takeichi, M. (1998). Dynamic behavior of the cadherin-based cell-cell adhesion system during Drosophila gastrulation. *Dev. Biol.* **203**, 435-450. doi:10.1006/dbio.1998.9047

O'Leary, N. A., Wright, M. W., Brister, J. R., Ciufo, S., Haddad, D., McVeigh, R., Rajput, B., Robbertse, B., Smith-White, B., Ako-Adjei, D. et al. (2016). Reference sequence (RefSeq) database at NCBI: current status, taxonomic expansion, and functional annotation. *Nucleic Acids Res.* **44**, D733-D745. doi:10.1093/nar/gkv1189

Pla, P., Moore, R., Morali, O. G., Grille, S., Martinozzi, S., Delmas, V. and Larue, L. (2001). Cadherins in neural crest cell development and transformation. *J. Cell. Physiol.* **189**, 121-132. doi:10.1002/jcp.10008

Pukhlyakova, E., Aman, A. J., Elsayad, K. and Technau, U. (2018). β-Catenin-dependent mechanotransduction dates back to the common ancestor of Cnidaria and Bilateria. *Proc. Natl. Acad. Sci. USA* **115**, 6231-6236. doi:10.1073/pnas.1713682115

Putnam, N. H., Srivastava, M., Hellsten, U., Dirks, B., Chapman, J., Salamov, A., Terry, A., Shapiro, H., Lindquist, E., Kapitonov, V. V. et al. (2007). Sea anemone genome reveals ancestral Eumetazoan Gene Repertoire and Genomic Organization. *Science* **317**, 86-94. doi:10.1126/science.1139158

Rachamim, T., Morgenstern, D., Aharonovich, D., Brekhman, V., Lotan, T. and Sher, D. (2015). The dynamically evolving nematocyst content of an anthozoan, a scyphozoan, and a hydrozoan. *Mol. Biol. Evol.* **32**, 740-753. doi:10.1093/molbev/msu335

Ragkousi, K., Marr, K., McKinney, S., Ellington, L. and Gibson, M. C. (2017). Cell-cycle-coupled oscillations in apical polarity and intercellular contact maintain order in embryonic epithelia. *Curr. Biol.* **27**, 1381-1386. doi:10.1016/j.cub.2017.03.064

Renfer, E., Amon-Hassenzahl, A., Steinmetz, P. R. H. and Technau, U. (2010). A muscle-specific transgenic reporter line of the sea anemone, *Nematostella vectensis*. *Proc. Natl. Acad. Sci. USA* **107**, 104-108. doi:10.1073/pnas.0909148107

Rentzsch, F., Fritzenwanker, J. H., Scholz, C. B. and Technau, U. (2008). FGF signalling controls formation of the apical sensory organ in the cnidarian *Nematostella vectensis*. *Development* **135**, 1761-1769. doi:10.1242/dev.020784

Rogers, C. D., Saxena, A. and Bronner, M. E. (2013). Sip1 mediates an E-cadherin-to-N-cadherin switch during cranial neural crest EMT. *J. Cell Biol.* **203**, 835-847. doi:10.1083/jcb.201305050

Röper, J.-C., Mitrossilis, D., Stirnemann, G., Waharte, F., Brito, I., Fernandez-Sanchez, M.-E., Baaden, M., Salamero, J. and Farge, E. (2018). The major β-catenin/E-cadherin junctional binding site is a primary molecular mechanotransductor of differentiation in vivo. *eLife* **7**, e33381. doi:10.7554/eLife.33381

Salinas-Saavedra, M., Rock, A. Q. and Martindale, M. Q. (2018). Germ layer-specific regulation of cell polarity and adhesion gives insight into the evolution of mesoderm. *eLife* **7**, 1438. doi:10.7554/eLife.36740

Scarpa, E., Szabó, A., Bibonne, A., Theveneau, E., Parsons, M. and Mayor, R. (2015). Cadherin switch during EMT in neural crest cells leads to contact inhibition of locomotion via repolarization of forces. *Dev. Cell* **34**, 421-434. doi:10.1016/j.devcel.2015.06.012

Schäfer, G., Narasimha, M., Vogelsang, E. and Leptin, M. (2014). Cadherin switching during the formation and differentiation of the Drosophila mesoderm - implications for epithelial-to-mesenchymal transitions. *J. Cell Sci.* **127**, 1511-1522. doi:10.1242/jcs.139485

Schindelin, J., Arganda-Carreras, I., Frise, E., Kaynig, V., Longair, M., Pietzsch, T., Preibisch, S., Rueden, C., Saalfeld, S., Schmid, B. et al. (2012). Fiji: an open-source platform for biological-image analysis. *Nat. Meth.* **9**, 676-682. doi:10.1038/nmeth.2019

Schneider, V. A., Graves-Lindsay, T., Howe, K., Bouk, N., Chen, H.-C., Kitts, P. A., Murphy, T. D., Pruitt, K. D., Thibaud-Nissen, F., Albracht, D. et al. (2017). Evaluation of GRCh38 and de novo haploid genome assemblies demonstrates the enduring quality of the reference assembly. *Genome Res.* **27**, 849-864. doi:10.1101/gr.213611.116

Scholz, C. B. and Technau, U. (2003). The ancestral role of Brachyury: expression of NemBra1 in the basal cnidarian *Nematostella vectensis* (Anthozoa). *Dev. Genes Evol.* **212**, 563-570. doi:10.1007/s00427-002-0214-7

Seybold, A., Salvenmoser, W. and Hobmayer, B. (2016). Sequential development of apical-basal and planar polarities in aggregating epitheliomuscular cells of Hydra. *Dev. Biol.* **412**, 148-159. doi:10.1016/j.ydbio.2016.02.022

Shimizu, T., Yabe, T., Muraoka, O., Yonemura, S., Aramaki, S., Hatta, K., Bae, Y.-K., Nojima, H. and Hibi, M. (2005). E-cadherin is required for gastrulation cell movements in zebrafish. *Mech. Dev.* **122**, 747-763. doi:10.1016/j.mod.2005.03.008

Shinzato, C., Shoguchi, E., Kawashima, T., Hamada, M., Hisata, K., Tanaka, M., Fujie, M., Fujiwara, M., Koyanagi, R., Ikuta, T. et al. (2011). Using the Acropora digitifera genome to understand coral responses to environmental change. *Nature* **476**, 320-323. doi:10.1038/nature10249

Shoval, I., Ludwig, A. and Kalcheim, C. (2007). Antagonistic roles of full-length N-cadherin and its soluble BMP cleavage product in neural crest delamination. *Development* **134**, 491-501. doi:10.1242/dev.02742

Steinmetz, P. R. H., Aman, A., Kraus, J. E. M. and Technau, U. (2017). Gut-like ectodermal tissue in a sea anemone challenges germ layer homology. *Nat. Ecol. Evol.* **1**, 1535-1542. doi:10.1038/s41559-017-0285-5

Technau, U. and Steele, R. E. (2011). Evolutionary crossroads in developmental biology: Cnidaria. *Development* **138**, 1447-1458. doi:10.1242/dev.048959

Thurmond, J., Goodman, J. L., Strelets, V. B., Attrill, H., Gramates, L. S., Marygold, S. J., Matthews, B. B., Millburn, G., Antonazzo, G., Trovisco, V. et al. (2019). FlyBase 2.0: the next generation. *Nucleic Acids Res.* **47**, D759-D765. doi:10.1093/nar/gky1003

Tucker, R. P. and Adams, J. C. (2014). Adhesion networks of cnidarians: a postgenomic view. *Int. Rev. Cell Mol. Biol.* **308**, 323-377. doi:10.1016/B978-0-12-800097-7.00008-7

Voolstra, C. R., Li, Y., Liew, Y. J., Baumgarten, S., Zoccola, D., Flot, J.-F., Tambutté, S., Allemand, D. and Aranda, M. (2017). Comparative analysis of the genomes of Stylophora pistillata and Acropora digitifera provides evidence for extensive differences between species of corals. *Sci. Rep.* **7**, 17583-17514. doi:10.1038/s41598-017-17484-x

Williams, E. J., Furness, J., Walsh, F. S. and Doherty, P. (1994). Activation of the Fgf receptor underlies neurite outgrowth stimulated by L1, N-Cam, and N-Cadherin. *Neuron* **13**, 583-594. doi:10.1016/0896-6273(94)90027-2

Winklbauer, R. (2012). Cadherin function during Xenopus gastrulation. In *Adherens Junctions: from Molecular Mechanisms to Tissue Development and Disease (Harris, T.J.C., ed.)*, pp. 301-320. Dordrecht: Springer Netherlands.

Zerbino, D. R., Achuthan, P., Akanni, W., Amode, M. R., Barrell, D., Bhai, J., Billis, K., Cummins, C., Gall, A., Girón, C. G. et al. (2018). Ensembl 2018. *Nucleic Acids Res.* **46**, D754-D761. doi:10.1093/nar/gkx1098